Journal of Virology

High, Broad, Polyfunctional, and Durable T Cell Immune Responses Induced in Mice by a Novel Hepatitis C Virus (HCV) Vaccine Candidate (MVA-HCV) Based on Modified Vaccinia Virus Ankara Expressing the Nearly Full-Length HCV Genome

Carmen E. Gómez, Beatriz Perdiguero, María Victoria Cepeda, Lidia Mingorance, Juan García-Arriaza, Andrea Vandermeeren, Carlos Óscar S. Sorzano and Mariano Esteban

J. Virol. **2013, 87(13):7282. DOI: 10.1128/JVI.03246-12. Published Ahead of Print 17 April 2013.**

JVI Journals.ASM.org

High, Broad, Polyfunctional, and Durable T Cell Immune Responses Induced in Mice by a Novel Hepatitis C Virus (HCV) Vaccine Candidate (MVA-HCV) Based on Modified Vaccinia Virus Ankara Expressing the Nearly Full-Length HCV Genome

Carmen E. Gómez,[a] Beatriz Perdiguero,[a] María Victoria Cepeda,[a] Lidia Mingorance,[a] Juan García-Arriaza,[a] Andrea Vandermeeren,[a]* Carlos Óscar S. Sorzano,[b] Mariano Esteban[a]

Department of Molecular and Cellular Biology, Centro Nacional de Biotecnología, Consejo Superior de Investigaciones Científicas, Madrid, Spain[a]; Biocomputing Unit, Centro Nacional de Biotecnología, Consejo Superior de Investigaciones Científicas, Madrid, Spain[b]

A major goal in the control of hepatitis C infection is the development of a vaccine. Here, we have developed a novel HCV vaccine candidate based on the highly attenuated poxvirus vector MVA (referred to as MVA-HCV) expressing the nearly full-length (7.9-kbp) HCV sequence, with the aim to target almost all of the T and B cell determinants described for HCV. In infected cells, MVA-HCV produces a polyprotein that is subsequently processed into the structural and nonstructural HCV proteins, triggering the cytoplasmic accumulation of dense membrane aggregates. In both C57BL/6 and transgenic HLA-A2-vaccinated mice, MVA-HCV induced high, broad, polyfunctional, and long-lasting HCV-specific T cell immune responses. The vaccine-induced T cell response was mainly mediated by CD8 T cells; however, although lower in magnitude, the $CD4^+$ T cells were highly polyfunctional. In homologous protocol (MVA-HCV/MVA-HCV) the main $CD8^+$ T cell target was p7+NS2, whereas in heterologous combination (DNA-HCV/MVA-HCV) the main target was NS3. Antigenic responses were also detected against other HCV proteins (Core, E1-E2, and NS4), but the magnitude of the responses was dependent on the protocol used. The majority of the HCV-induced $CD8^+$ T cells were triple or quadruple cytokine producers. The MVA-HCV vaccine induced memory $CD8^+$ T cell responses with an effector memory phenotype. Overall, our data showed that MVA-HCV induced broad, highly polyfunctional, and durable T cell responses of a magnitude and quality that might be associated with protective immunity and open the path for future considerations of MVA-HCV as a prophylactic and/or therapeutic vaccine candidate against HCV.

More than 170 million people are infected with hepatitis C virus (HCV) worldwide, and each year 3 million people are newly infected (1). Twenty percent of infected people eliminate the virus over the weeks or months following an acute infection and are frequently asymptomatic. The remaining 80% will develop chronic disease and, of these, nearly 20% of the chronic patients ultimately develop liver cirrhosis and 1 to 5% will develop liver cancer (2, 3).

The standard-of-care treatment for patients infected with HCV is a combination of pegylated interferon-α and ribavirin. This treatment is long, displays a broad side effect profile, commonly fails, and is prohibitively expensive in developing countries (4). A major effort has been directed to the development of new antiviral agents. Direct-acting antivirals in clinical development include NS3-4A protease inhibitors, two of which, telaprevir and boceprevir, have recently been approved for the treatment of HCV genotype 1 infection in combination with pegylated interferon-α and ribavirin, nucleoside/nucleotide analogue, and non-nucleoside inhibitors of HCV RNA-dependent RNA polymerase and NS5A inhibitors, as well as host target agents (5). Due to the cost, side effects, and complex treatments, as well as the development of HCV-resistant mutants and viral heterogeneity, antiviral therapy is not the solution to eradicate HCV infection. Hence, there is an urgent need to develop an effective prophylactic vaccine.

The observation that a significant percentage of acutely infected patients spontaneously eliminate the virus together with a potent antiviral immunity suggests that the development of a prophylactic vaccine is a feasible aim. The comparison of hosts who spontaneously eradicate HCV to those who develop chronic disease has permitted the characterization of innate and adaptive immune processes that are relevant in the outcome of infection (6).

The role of HCV-specific T cell responses in the outcome of primary HCV infection has been widely studied, and although a single correlate of protection has not been determined, it is known that this arm of the immune response is determinant in the clearance of the virus. There are several lines of evidence that support this remark. First, comparative studies in humans have shown that wide and long-lasting $CD8^+$ and $CD4^+$ T cell responses against multiple HCV regions are related to spontaneous viral clearance. On the other hand, a low and limited HCV-specific T cell response is a hallmark of chronic infection (7–9). Second, immunogenicity studies derived from mixed populations and single-source outbreaks have demonstrated a clear association between specific HLA class I and II alleles and viral clearance (10). Both HLA-A3 and HLA-B27 alleles were reported to be protective against the

Received 21 November 2012 **Accepted** 4 April 2013
Published ahead of print 17 April 2013
Address correspondence to Mariano Esteban, mesteban@cnb.csic.es.
* Present address: Andrea Vandermeeren, Chiltern International, Tres Cantos, Madrid, Spain.

doi:10.1128/JVI.03246-12

development of persistent infection after an outbreak of HCV from genotype 1b infection in Irish women in 1977. Third, in the chimpanzee model it has been shown that once protective responses are triggered, depletion of either $CD4^+$ and $CD8^+$ T cells results in the loss of control over recurrent HCV challenges (11).

The protective role of HCV antibodies is still controversial. It has been shown that antibody-deficient patients can recover from acute HCV infection in the absence of anti-HCV antibodies (12). However, a strong line of evidence now exists demonstrating that neutralizing antibody responses to epitopes in the viral E1 and E2 glycoproteins can be protective (13) and are associated with the resolution of hepatitis C infection (14). Moreover, it has been recently described that human liver-chimeric mice (Alb-uPA/SCID) injected with neutralizing antibodies derived from patients with chronic infection were protected from homologous (15, 16) or heterologous (17) HCV challenges.

Based on the virus-host interactions during HCV infection, there are three characteristics likely to be shared by successful prophylactic and therapeutic vaccine candidates. First, these vaccines need to elicit a potent, wide, and functional T cell response and also a humoral immune response to a broad array of HCV antigens. Second, they will target relatively conserved viral regions to counteract with the high levels of viral genetic diversity between and within hosts. Third, they need to eliminate HCV from the liver without producing liver immunopathology in order to be safe.

Peptide, recombinant protein, DNA, and vector-based vaccines have all been examined with different degrees of success as preventive and therapeutic HCV vaccine candidates (6, 18, 19). Recombinant protein vaccines that trigger anti-envelope humoral responses are not likely to generate sterilizing immunity due to the genetic variability of the HCV envelope region but may yet have a role in the attenuation of the course of primary infection or function as an adjuvant to a T cell-based vaccine. Peptide- and protein-based T cell vaccines have been shown to induce low T cell responses, and thus this strategy will only progress with the development of novel adjuvants. DNA vaccines, with supplementary techniques to increase delivery and immunogenicity, have demonstrated some promising results and have been reported to reduce viral load in some persistently infected patients (6, 18, 19). The most promising observations have been derived from the use of viral vector-based vaccines, such as replication-defective adenovirus or modified vaccinia virus Ankara (MVA). Adenoviral vectors expressing nonstructural proteins from genotype 1b have been shown to be highly immunogenic in healthy volunteers (20). Nevertheless, the effects of these vectors in HCV-infected patients are not yet known. In the same way, MVA-based HCV vaccine candidates targeting structural and/or nonstructural HCV proteins have also been shown to elicit high quality T cell immune responses in preclinical (21–24) and clinical (25) studies. The most advanced therapeutic studies using MVA have been conducted with the TG4040 candidate. It is a recombinant poly-antigenic T cell vaccine based on MVA that encodes NS3, NS4, and NS5B HCV proteins. HCV-specific T cell responses were detected in all patients as early as 1 week after the first vaccination and were maintained during the 6-month follow-up. Vaccination reduced HCV viral loads by up to 1.5 $\log_{10}$, and the strongest vaccine specific T cell responses were observed in patients who achieved the greatest viral load reductions (25). In addition, a randomized phase II study involving 153 patients in three treatment groups is currently ongoing. Preliminary data published on the website of Transgene show a reduction of viral load as early as 1 week after the initiation of standard-of-care treatment in the group prevaccinated with TG4040 prior to the introduction of the treatment, which is faster than in both other groups receiving the standard-of-care treatment alone or a combination of the standard-of-care treatment with TG4040 in the same treatment schedule (http://www.clinicaltrials.gov, NCT01055821).

Because current HCV candidate vaccines are designed to target a limited number of viral antigens, we decided to develop a new vaccine candidate based on the attenuated MVA strain that constitutively expresses a nearly full-length HCV genome from genotype 1a (MVA-HCV). This HCV open reading frame (ORF) was previously used for the generation of the recombinant vaccinia virus vT7-$HCV_{7.9}$ from the virulent WR strain that, upon induction with IPTG (isopropyl-β-D-thiogalactopyranoside), is efficiently transcribed into a polyprotein precursor that is correctly processed into mature structural proteins (Core, E1, and E2), viroporin p7 protein, and nonstructural proteins (NS2, NS3, NS4A, NS4B, NS5A, and part of NS5B) (26). For safety reasons, the HCV polyprotein encoded by MVA-HCV recombinant virus only contains the first 201 amino acids of the nonstructural protein 5B (NS5B). NS5B is considered to possess RNA-dependent RNA polymerase (RdRp) activity and to play an essential role in viral replication. It works in a membrane-associated complex that also contains NS3, NS4A, NS4B, and NS5A (27). NS5B is anchored to the membranes via a C-terminal 20-amino-acid hydrophobic domain. These residues are dispensable for enzymatic activity but needed for viral replication in cells (28). The removal of almost 70% of NS5B protein that abrogates its enzymatic activity, and its interaction with the replication complex, together with the absence of 5′- and 3′-NTRs that contain important *cis*-acting regulatory sequences, assure that during a coinfection of HCV and MVA-HCV vaccine the viral insert cannot contribute to generate a replication-competent HCV.

In an effort to develop HCV vaccine candidates, we describe here the generation, characterization, and preclinical evaluation of MVA-HCV that constitutively expresses all of the HCV proteins (except the C-terminal region of NS5B). We specifically addressed the breadth, phenotype, polyfunctionality, and longevity of the vaccine-elicited immune responses in mice in order to provide insights into the immune potential of MVA-HCV administered in homologous or heterologous regimens as candidate vaccine.

MATERIALS AND METHODS

Ethics statement. The animal studies were approved by the Ethical Committee of Animal Experimentation (CEEA-CNB) of Centro Nacional de Biotecnologia (CNB-CSIC; Madrid, Spain) in accordance with national and international guidelines and with the Royal Decree (RD 1201/2005 [permit number 11048]).

Cells and viruses. BHK-21 cells (baby hamster kidney fibroblasts, American Type Culture Collection [ATCC] catalog no. CCL-10), DF-1 cells (a spontaneously immortalized chicken embryo fibroblast (CEF) cell line, ATCC catalog no. CRL-12203), and HeLa cells (a human epithelial cervix adenocarcinoma, ATCC catalog no. CCL-2) were grown in Dulbecco modified Eagle medium (DMEM) supplemented with 100 IU of penicillin/ml, 100 μg of streptomycin/ml, and 10% fetal calf serum (FCS). Human HepG2 hepatocellular carcinoma cells (ATCC catalog no. HB-8065) were maintained in DMEM supplemented with penicillin (100 IU/ml), streptomycin (100 μg/ml), glutamine (2 mM), HEPES buffer (pH

7.4; 20 mM), and 10% FCS. Human monocyte-derived dendritic cells (DCs) were obtained from freshly isolated peripheral blood mononuclear cells by Ficoll gradient separation on Ficoll-Paque (GE Healthcare) from buffy coats of healthy blood donors (recruited by the Centro de Transfusión de la Comunidad de Madrid, Madrid, Spain). Then, $CD14^+$ monocytes were purified by depletion using Dynabeads Untouched human monocytes kit (Invitrogen), following the manufacturer's recommendations. The obtained monocytes were cultured for 7 days in six-well culture plates (3×10^6 cells/well at 1×10^6 cells/ml) in complete RPMI 1640 medium containing 10% FCS and supplemented with 50 ng of granulocyte-macrophage colony-stimulating factor/ml and 20 ng of interleukin-4 (IL-4)/ml (both from Gibco-Life Technologies). The purity of sorted DC populations was >99%. The human monocytic THP-1 cell line (ATCC catalog no. TIB-202) was cultured in complete RPMI 1640 medium containing 2 mM L-glutamine, 50 mM 2-mercaptoethanol, 100 IU of penicillin/ml, 100 μg of streptomycin/ml, and 10% FCS. THP-1 cells were differentiated into macrophages by treatment with 0.5 mM phorbol 12-myristate 13-acetate (PMA; Sigma-Aldrich) for 24 h before usage. Cells were maintained in a humidified air–5% CO_2 atmosphere at 37°C (or 39°C for the DF-1 cell line). Virus infections were performed with 2% FCS.

The poxvirus strain used in the present study as the parental virus for the generation of the recombinant virus MVA-HCV is the modified vaccinia virus Ankara (MVA) obtained from the Ankara strain after 586 serial passages in CEF cells (derived from clone F6 at passage 585, kindly provided by G. Sutter, Germany). Both viruses were grown in BHK-21 cells, similarly purified through two 36% (wt/vol) sucrose cushions, and titrated by immunostaining plaque assay as previously described (29). The titration of the different viruses was performed at least three times.

Construction of plasmid transfer vector pCyA-HCV$_{7.9}$. A 7.9-kbp DNA fragment encoding the structural (C, E1, and E2), the viroporin p7 and nonstructural (NS2, NS3, NS4A, NS4B, and NS5A, plus 201 amino acids of the N-terminal region of NS5B) proteins of HCV virus H77 from genotype 1a was excised with EcoRI from the original full-length HCV genome containing plasmid pHCV1a (kindly provided by Charles M. Rice, New York, NY). The 5′- and 3′-NTR regions of HCV genome are not part of the construct. This DNA fragment was treated with Klenow enzyme (Roche) to generate blunt ends and cloned into the VACV insertion vector pCyA-20 previously digested with PmeI and dephosphorylated by incubation with shrimp alkaline phosphatase (USB) to generate the plasmid transfer vector pCyA-HCV$_{7.9}$ (see Fig. 1A). The plasmid pCyA-20, used for the generation of plasmid pCyA-HCV$_{7.9}$, was constructed by the insertion of a synthetic band containing the viral early/late promoter and a multiple cloning site into the plasmid pLZAW1 (provided by Sanofi-Pasteur). The synthetic band was obtained by the annealing of two complementary oligonucleotides (88 bp each) containing AscI and SwaI restriction sites (underlined): 5′-AGGCGCGCCAAAAATTGAAATTTTATTTTTTTTTTTGGAATATAAATAGCTAGCTCGAGTTTAAACTGCAGAGATCTATTTAAATCC-3′ and 5′-GGATTTAAATAGATCTCTGCAGTTTAAACTCGAGCTAGCTATTTATATTCCAAAAAAAAAAAAATAAAATTTCAATTTTTGGCGCGCCT-3′. This synthetic band was digested with AscI and SwaI and cloned into pLZAW1 previously digested with the same restriction enzymes to generate plasmid pCyA-20.

The resulting plasmid transfer vector, pCyA-HCV$_{7.9}$, was confirmed by DNA sequence analysis and directs the insertion of HCV genes into the TK locus of the MVA-WT genome under the transcriptional control of the viral synthetic early/late (sE/L) promoter. It contains a β-Gal reporter gene sequence between two repetitions of the left TK flanking arm, which allows the reporter gene to be deleted from the final recombinant virus by homologous recombination after successive passages.

Construction of MVA-HCV recombinant virus. BHK-21 cells (3×10^6 cells) were infected with MVA-WT at a multiplicity of 0.01 PFU/cell and transfected 1 h later with 10 μg of DNA of plasmid pCyA-HCV$_{7.9}$, using Lipofectamine reagent according to the manufacturer's recommendations (Invitrogen). After 72 h postinfection (hpi), the cells were harvested, lysed by freeze-thaw cycling, sonicated, and used for recombinant virus screening. Recombinant MVA viruses containing the 7.9-kb HCV1a DNA fragment and transiently coexpressing the β-Gal marker gene (MVA-HCV, X-Gal$^+$) were selected by consecutive rounds of plaque purification in BHK-21 cells stained with X-Gal (5-bromo-4-chloro-3-indolyl-β-D-galactopyranoside; 400 μg/ml, four passages in total). In the following plaque purification steps, recombinant MVA viruses containing HCV1a DNA fragment and having deleted the β-Gal gene by homologous recombination between the TK left arm and the short TK left arm repeat flanking the marker (MVA-HCV, X-Gal$^-$) were isolated by three additional consecutive rounds of plaque purification screening for nonstaining viral foci in BHK-21 cells in the presence of X-Gal (400 μg/ml). In each round of purification, the isolated plaques were expanded in BHK-21 cells for 3 days, and crude viruses obtained were used for the next plaque purification round. The resulting MVA-HCV recombinant virus was grown in BHK-21 cells, purified through two 36% (wt/vol) sucrose cushions, and titrated by immunostaining plaque assay. Purity of the recombinant virus was confirmed by PCR with primers spanning the junction regions of the HCV1a insert and by DNA sequence analysis.

PCR analysis of MVA-HCV recombinant virus. To test the identity and purity of the recombinant virus MVA-HCV, viral DNA was extracted from BHK-21 cells infected at 5 PFU/cell with MVA-WT or MVA-HCV. Cell membranes were disrupted using sodium dodecyl sulfate (SDS), followed by proteinase K treatment (0.2 mg of proteinase K/ml in 50 mM Tris-HCl [pH 8], 100 mM EDTA [pH 8], 100 mM NaCl, and 1% SDS for 1 h at 55°C) and phenol extraction of viral DNA. Primers TK-L (5′-TGATTAGTTTGATGCGATTC-3′) and TK-R (5′-TGTCCTTGATACGGCAG-3′) annealing in the TK flanking sequences (Fig. 1B) were used for PCR analysis of TK locus. The amplification reactions were performed with Platinum *Taq* DNA polymerase (Invitrogen) according to the manufacturer's recommendations.

Analysis of virus growth. To determine virus growth profiles, monolayers of BHK-21 cells grown in 12-well plates were infected in duplicate at 0.01 PFU/cell with MVA-WT or MVA-HCV recombinant virus. After virus adsorption for 60 min at 37°C, the inoculum was removed. The infected cells were washed once with DMEM without serum and incubated with fresh DMEM containing 2% FCS at 37°C in a 5% CO_2 atmosphere. At different times postinfection (0, 24, 48, and 72 h), cells were harvested by scraping (lysates at 5×10^5 cells/ml), freeze-thawed three times, and briefly sonicated. Virus titers in cell lysates were determined by immunostaining assay in chick DF-1 cells using rabbit polyclonal anti-vaccinia virus strain WR (Centro Nacional de Biotecnología; diluted 1:1,000), followed by anti-rabbit-HRPO (Sigma; diluted 1:1,000).

Expression of HCV proteins from MVA-HCV recombinant virus by Western blot analysis. To test the correct expression of HCV antigens by the MVA-HCV recombinant virus, monolayers of BHK-21 cells were mock infected or infected at 5 PFU/cell with MVA-WT or MVA-HCV. At 24 h postinfection, cells were lysed in Laemmli buffer, and cell extracts were fractionated by SDS–12% PAGE and analyzed by Western blotting with rabbit polyclonal antibody against Core (kindly provided by Ilkka Julkunen; National Public Health Institute, Finland; diluted 1:1,000), mouse monoclonal antibodies against E1 (Acris Antibodies; diluted 1:1,000), E2 (GenWay Biotech; diluted 1:500), NS4A, NS4B, and NS5A (all from GenWay Biotech; diluted 1:1000), or goat polyclonal antibody against NS3 (Abcam; diluted 1:500, kindly provided by Pablo Gastaminza) to evaluate the expression of the different HCV proteins. The anti-rabbit-HRPO diluted 1:5,000 (Sigma), anti-mouse-HRPO diluted 1:2,000 (Sigma), or anti-goat-HRPO diluted 1:100,000 (Sigma) were used as secondary antibodies. The immunocomplexes were detected by enhanced chemiluminescence (GE Healthcare).

Expression of HCV proteins from MVA-HCV recombinant virus by confocal immunofluorescence microscopy analysis. HeLa cells cultured on glass coverslips at a confluence of 50% were mock infected or infected with MVA-WT or MVA-HCV at a multiplicity of infection (MOI) of 0.5 PFU/cell. At 16 h postinfection, the cells were washed with phosphate-

buffered saline (PBS) and fixed with 3% paraformaldehyde (PFA) in PBS at room temperature for 15 min. Cells were quenched for 15 min in the presence of 50 mM NH_4Cl and permeabilized and blocked with 0.05% saponin–5% FCS in PBS. Mouse monoclonal antibodies against HCV proteins E1 (Acris Antibodies) or NS5A (GenWay), rabbit polyclonal antibody against HCV protein NS4B (kindly provided by Ilkka Julkunen), and mouse monoclonal anti-PDI or rabbit polyclonal anti-calnexin antibodies (BioNova), both against endoplasmic reticulum (ER), were used to stain the cells for 1 h at room temperature in the presence of 0.05% saponin–5% FCS in PBS, followed by washing with PBS and 1 h of incubation in the dark at room temperature with specific mouse or rabbit secondary antibodies conjugated with the fluorochromes Alexa 488 (green) or Alexa 594 (red) (Invitrogen). Coverslips were then washed with PBS, and cell nuclei were stained with DAPI (4′,6′-diamidino-2-phenylindole; Sigma) in PBS. After staining, coverslips were conserved in ProLong Gold antifade reagent, and optical sections of the cells were examined using a Leica TCS SP5 microscope. Images were recorded and processed by use of the specialized software LasAF (Leica Microsystems).

Electron microscopy analysis. Confluent HeLa cells growing on 60-cm^2 plastic culture dishes were infected with MVA-WT or MVA-HCV at an MOI of 5 PFU/cell. At 16 hpi, cells were fixed for 2 h at room temperature in 2% glutaraldehyde–1% tannic acid in 0.4 M HEPES buffer (pH 7.2) and then collected by careful scraping. Cellular pellet was washed in HEPES buffer, followed by conventional embedding in the epoxy-resin EML-812 (Taab Laboratories) as previously described (30). Ultrathin sections of 70 nm were cut from the embedded pellet, collected on copper grids, and examined with a JEOL 1011 transmission electron microscope. All images were recorded with an ES1000W Erlangshen charge-coupled device camera (Gatan).

Time course expression of HCV proteins from MVA-HCV recombinant virus. BHK-21 or HepG2 cells grown in 12-well culture plates were mock infected or infected at 5 PFU/cell with MVA-WT or MVA-HCV recombinant virus. At different hours postinfection, the cells were collected and centrifuged at 1,500 rpm for 10 min, and cellular pellets were lysed in Laemmli buffer containing β-mercaptoethanol. Cell extracts were fractionated by SDS–12% PAGE and analyzed by Western blotting with an HCV antibody-positive human serum (diluted 1:500), followed by anti-human-HRPO (Sigma; diluted 1:1,000) to evaluate the expression of HCV proteins. The immunocomplexes were detected by enhanced chemiluminescence (GE Healthcare).

Genetic stability of MVA-HCV recombinant virus by expression analysis. Monolayers of BHK-21 cells were infected at 0.05 PFU/cell with MVA-HCV recombinant virus. At 72 hpi, cells were collected by scraping. After three freeze-thaw cycles and brief sonication, the cellular extract was centrifuged at 1,500 rpm for 5 min, and the supernatant was used for a new round of infection at 0.05 PFU/cell. The same procedure was repeated four times. Expression of HCV proteins at all four passages was detected by Western blot after infection of BHK-21 cells with virus stocks from each passage using an HCV antibody-positive human sera (kindly provided by Rafael Fernández from Hospital Ramón y Cajal, Madrid, Spain; diluted 1:500). Anti-human-HRPO diluted 1:1,000 (Sigma) was used as a secondary antibody. The immunocomplexes were detected by enhanced chemiluminescence (GE Healthcare).

The stability of the MVA-HCV recombinant virus was also evaluated in individual plaques. Monolayers of BHK-21 cells grown in six-well plates were infected with serial dilutions of cell lysates at passage 4 from MVA-HCV infections. After 1 h of virus adsorption, the virus inoculum was removed, and the cells were overlaid with agar. At 48 hpi, the cells were stained with 0.01% neutral red (Sigma), and 15 h later 30 individual plaques were picked up, resuspended in 0.5 ml of DMEM, freeze-thawed three times, and briefly sonicated. Then, 0.2 ml of each plaque was used for infection of BHK-21 cells in 24-well plates. At 72 hpi, the cells were lysed in Laemmli buffer containing β-mercaptoethanol, and cell extracts were fractionated by SDS–12% PAGE and analyzed by Western blotting with HCV antibody-positive human sera (diluted 1:500), followed by anti-human-HRPO (Sigma; diluted 1:1,000) to evaluate the expression of HCV proteins. The immunocomplexes were detected by enhanced chemiluminescence (GE Healthcare).

RNA analysis by quantitative real-time PCR. Total RNA was isolated by using the RNeasy kit (Qiagen) from DCs mock infected or infected at 0.3 or 1 PFU/cell with MVA-WT or MVA-HCV for 6 h. Reverse transcription of 500 ng of RNA was performed by using a QuantiTect reverse transcription kit (Qiagen). Quantitative PCR was performed with a 7500 real-time PCR system (Applied Biosystems) using the Power SYBR green PCR Master Mix (Applied Biosystems), as previously described (31). The expression levels of *IFN-β*, *IFIT1*, *IFIT2*, *RIG-I*, *MDA-5*, *IP-10*, and *HPRT* genes were analyzed by real-time PCR using specific oligonucleotides (the sequences are available from the authors upon request). Gene-specific expression was expressed relative to the expression of *HPRT* in arbitrary units. All samples were tested in duplicate, and two different experiments were performed.

Analysis of IRF3 phosphorylation by Western blotting. The phosphorylation of IRF-3 was analyzed by Western blotting in extracts from THP-1 cells mock infected or infected with MVA-WT or MVA-HCV at 5 PFU/cell. At different times postinfection (45 min, 90 min, 3 h, or 6 h), cells were harvested, and protein extracts were obtained using lysis buffer according to the manufacturer's recommendations (cell lysis buffer; Cell Signaling). Equal amounts of protein (30 μg) were fractionated by SDS–10% PAGE and analyzed by Western blotting with rabbit monoclonal anti-P-IRF-3 (Cell Signaling; diluted 1:1,000) to evaluate the phosphorylation of IRF-3 or rabbit monoclonal anti-α-tubulin (Cell Signaling; diluted 1:2,000) as a loading control, followed by anti-rabbit-HRPO (Sigma; diluted 1:5,000). The immunocomplexes were detected by enhanced chemiluminescence (GE Healthcare).

DNA vectors. The DNA vaccine constructs pcDNA-Core, pcDNA-E1, pcDNA-E2, and pcDNA-NS3 were kindly provided by Ilkka Julkunen (National Public Health Institute, Finland). Plasmids were purified by using Maxi-Prep purification kits (Qiagen) and diluted for injection in endotoxin-free phosphate-buffered saline. The Core, E1, E2, and NS3 proteins encoded by these plasmids belong to HCV virus H77, genotype 1a.

Peptides. The HCV virus J4 (genotype 1b; GenPept no. AAC15722) peptide pools Core, E1, E2, p7+NS2, NS3-1, NS3-2, NS4, NS5-1, NS5-2, and NS5-3, with each purified peptide at 1 mg per vial, were obtained through BEI Resources, National Institute of Allergy and Infectious Disease, National Institutes of Health. They spanned the entire HCV1b proteins as consecutive 13- to 19-mers overlapped by 11 or 12 amino acids. Core protein was spanned by the Core peptide pool (28 peptides). E1 protein was spanned by the E1 pool (28 peptides). E2 protein was spanned by the E2 pool (55 peptides). The p7 and NS2 proteins were spanned by the p7+NS2 pool (40 peptides). NS3 protein was spanned by the following pools: NS3-1 (49 peptides) and NS3-2 (49 peptides). NS4 protein was spanned by the NS4 pool (47 peptides), and NS5 protein was spanned by the following pools: NS5-1 (55 peptides), NS5-2 (53 peptides), and NS5-3 (53 peptides). The HCV virus J4 genotype 1b shares an 85.7% of amino acid sequence homology with the HCV virus H77 genotype 1a.

C57BL/6 mice immunization schedule. C57BL/6 mice (6 to 8 weeks old) were purchased from Jackson Laboratory. For the homologous MVA prime-MVA boost immunization protocol performed to assay the immunogenicity of the MVA-HCV recombinant virus, groups of animals ($n = 8$) were immunized with 10^7 PFU of MVA-WT or MVA-HCV by the intraperitoneal (i.p.) route. Two weeks later, animals received 10^7 PFU of MVA-WT or MVA-HCV by the i.p. route. For the heterologous DNA prime-MVA boost immunization protocol, groups of animals ($n = 8$) received 200 μg of DNA-HCV (50 μg of pcDNA-Core plus 50 μg of pcDNA-E1 plus 50 μg of pcDNA-E2 plus 50 μg of pcDNA-NS3) or 200 μg of sham DNA (DNA-ϕ) (200 μg of pcDNA) by the intramuscular (i.m.) route. For DNA priming, we selected plasmid vectors expressing the HCV proteins Core, E1, E2, and NS3 since these antigens represent the main targets in the current HCV vaccine candidates (20–23). Two weeks later, animals were immunized with 10^7 PFU of MVA-WT or MVA-HCV

by the i.p. route. At 10 and 53 days after the last immunization, four mice in each group were sacrificed and spleens processed for intracellular cytokine staining (ICS) assay to measure the adaptive and memory cellular immune responses against HCV antigens, respectively. At 53 days after the last immunization, livers were processed by mechanical disruption as previously described (32) to measure, by ICS assay, the memory cellular immune response against HCV antigens in murine intrahepatic immune cells (IHICs).

C57BL/6-Tg(HLA-A2.1)1Enge/J mice immunization schedule. C57BL/6-Tg(HLA-A2.1)1Enge/J mice (6 to 8 weeks old) were purchased from Jackson Laboratory. This homozygous transgenic mice carrying the Tg(HLA-A2.1)1Enge transgene express significant quantities of the human class I MHC Ag HLA-A2.1 on cells from the spleen, bone marrow, and thymus. For the heterologous DNA prime-MVA boost immunization protocol, groups of animals ($n = 8$) received 200 μg of DNA-HCV (50 μg of pcDNA-Core plus 50 μg of pcDNA-E1 plus 50 μg of pcDNA-E2 plus 50 μg of pcDNA-NS3) or 200 μg of DNA-ϕ (200 μg of pcDNA) by the i.m. route. Two weeks later, animals were immunized with 10^7 PFU of MVA-WT or MVA-HCV by the i.p. route. At 10 and 53 days after the last immunization, four mice in each group were sacrificed, and the spleens were processed for ICS assay to measure the adaptive and memory cellular immune responses against HCV antigens, respectively.

ICS assay. The magnitude, polyfunctionality, and phenotype of the HCV-specific T cell responses were analyzed by ICS. After an overnight rest, 4×10^6 splenocytes or IHICs (depleted of red blood cells) were seeded on 96-well plates and stimulated for 6 h in complete RPMI 1640 medium supplemented with 10% FCS containing 1 μl of GolgiPlug (BD Biosciences)/ml, anti-CD107a-Alexa 488 (BD Biosciences), and 1 μg of the different HCV peptide pools/ml. At the end of the stimulation period, the cells were washed, stained for the surface markers, fixed, permeabilized (Cytofix/Cytoperm kit; BD Biosciences), and stained intracellularly using the appropriate fluorochromes. Dead cells were excluded by using the violet Live/Dead stain kit (Invitrogen). For functional analyses, the following fluorochrome-conjugated antibodies were used: CD3-PE-CF594, CD4-APC-Cy7, CD4-Alexa 700, CD8-V500, IFN-γ-PE-Cy7, IFN-γ-PerCP-Cy5.5, IL-2-APC, and TNF-α-PE (all from BD Biosciences). In addition, for phenotypic analyses, the following antibodies were used: CD62L-Alexa 700 or CD62L-APC (BD Biosciences) and CD127-PerCP-Cy5.5 (eBioscience). Cells were acquired using a Gallios flow cytometer (Beckman Coulter). Analyses of the data were performed using the FlowJo software version 8.5.3 (Tree Star, Ashland, OR). The number of lymphocyte-gated events ranged between 10^5 and 10^6. After gating, Boolean combinations of single functional gates were then created using FlowJo software to determine the frequency of each response based on all possible combinations of cytokine expression or all possible combinations of differentiation marker expression. Background responses detected in negative control samples were subtracted from those detected in stimulated samples for every specific functional combination.

Data analysis and statistics. For the statistical analysis of ICS data, we used a novel approach that corrects measurements for the medium response (RPMI) and allows the calculation of confidence intervals and *P* values of hypothesis tests (33, 34). Only antigen responses values significantly higher than the corresponding RPMI are represented, and the background for the different cytokines in the unstimulated controls never exceeded 0.05%. Analysis and presentation of distributions was performed using SPICE version 5.1 (http://exon.niaid.nih.gov) (35). Comparison of distributions was performed using a Student *t* test and a partial permutation test as described previously (35). All values used for analyzing proportionate representation of responses are background subtracted.

RESULTS

Generation and *in vitro* characterization of an MVA recombinant that constitutively expresses the nearly full-length HCV genome from genotype 1a (MVA-HCV). (i) Purity and virus growth of MVA-HCV recombinant virus. We have previously described the generation of the recombinant vaccinia virus vT7-$HCV_{7.9}$ from the virulent WR strain that, upon induction with IPTG, efficiently transcribed and translated a 7.9-kbp DNA fragment of the HCV ORF from genotype 1a into a polyprotein precursor that is correctly processed into mature structural and nonstructural HCV proteins (26).

Here we have generated the MVA-HCV, a recombinant based on the attenuated poxvirus strain MVA, that has inserted in the TK locus the same DNA fragment included in the vT7-$HCV_{7.9}$ vector but is now under the transcriptional control of the synthetic early/late viral promoter driving the constitutive expression of the structural and nonstructural HCV proteins. A diagram with the cloning steps for the construction of the plasmid transfer vector used for the generation of MVA-HCV is shown in Fig. 1A, and the organization of the HCV genome in the TK locus of MVA genome is shown in Fig. 1B.

The correct insertion and purity of MVA-HCV virus was confirmed by PCR and DNA sequence analysis. Viral DNA purified from BHK-21 cells infected with MVA-HCV was amplified using a set of primers annealing in the TK flanking sequences. The size of the expected PCR product is represented in Fig. 1B. DNA extracted from cells infected with the parental strain of MVA (MVA-WT) was used as control. As shown in Fig. 1C, the PCR product observed in cells infected with MVA-HCV has a full-length size of ~8 kbp, indicating that the HCV ORF was successfully inserted into the MVA TK locus and that no virus wild-type contamination was present in the virus preparation. This result was also confirmed by DNA sequence of viral TK locus.

To determine whether the expression of HCV proteins affects virus replication in cell culture, we next analyzed virus growth of MVA-HCV and MVA-WT in BHK-21 cells. As shown in Fig. 1D, the kinetics of viral growth were similar between parental and recombinant MVA-HCV viruses, indicating that the constitutive expression of HCV proteins does not impair vector replication under permissive conditions.

(ii) Correct expression of HCV proteins by MVA-HCV and cytoplasmic formation of dense membrane aggregates. To verify that MVA-HCV constitutively expresses and correctly processes the HCV polyprotein, we performed a Western blot analysis of BHK-21 cells infected with MVA-HCV or MVA-WT using specific antibodies that recognized the HCV Core, E1, E2, NS3, NS4A, NS4B, and NS5A proteins. As shown in Fig. 2A, the HCV ORF was efficiently transcribed during MVA-HCV infection, producing a viral polyprotein that is correctly processed into mature structural (Core, E1, and E2) and nonstructural (NS3, NS4A, NS4B, and NS5A) HCV proteins. Expression of p7 and NS2 proteins is not shown since we did not have specific antibodies. However, the fact that the polyprotein was correctly processed indicates that the other proteins should also be properly expressed by MVA-HCV.

The expression and intracellular localization of structural E1 and nonstructural NS4B and NS5A proteins was also confirmed by immunofluorescence analysis in HeLa cells using specific antibodies to HCV proteins, as well as specific antibodies for the cell ER (anti-calnexin and anti-PDI). As shown in Fig. 2B, there is a main appearance of these HCV proteins within globular and dense cytoplasmic structures, showing colocalization between HCV E1, NS4B and NS5A, and ER proteins.

Since we have previously observed that inducible expression of HCV proteins from WR strain induces specific morphological cell alterations (30), we next assayed the impact of HCV proteins con-

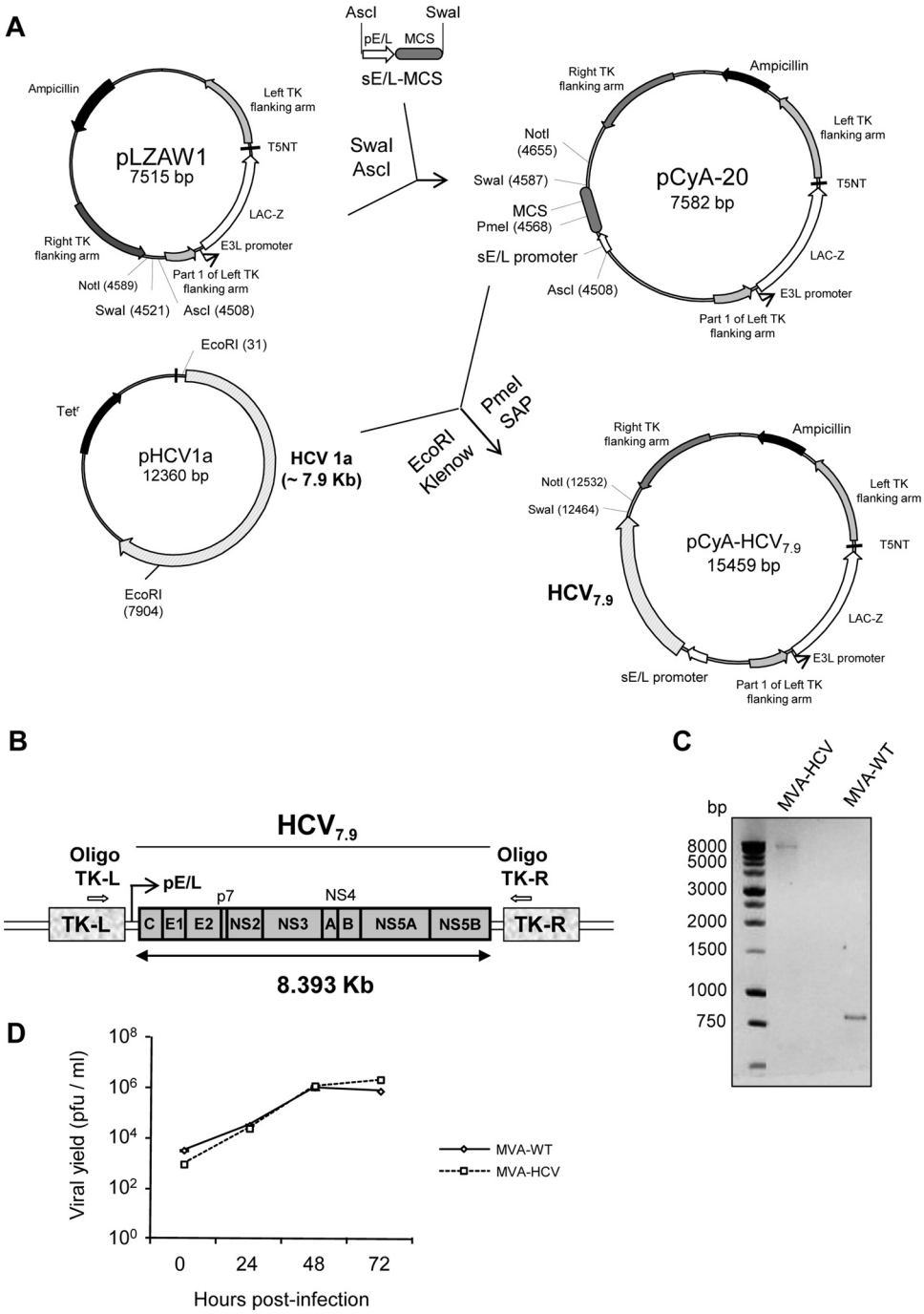

FIG 1 *In vitro* characterization of MVA-HCV recombinant virus. (A) Scheme of construction of the plasmid transfer vector pCyA-HCV$_{7.9}$. (B) Scheme of the organization of the HCV genome in the TK locus of MVA genome. (C) Confirmation of full-length HCV ORF insertion by PCR analysis. In parental MVA, a 873-bp product was obtained, whereas in recombinant virus a unique 8,393-bp product is observed. (D) Analysis of virus growth of MVA-HCV in BHK-21 cells. Monolayers of BHK-21 cells were infected with MVA-WT or MVA-HCV. At different times postinfection (0, 24, 48, and 72 h), the cells were collected, and infectious viruses were quantified by immunostaining assay of virus plaques.

stitutively expressed by MVA-HCV on HeLa cell architecture using transmission electron microscopy (EM) analysis. Ultrathin sections of HeLa cells infected with MVA-WT or MVA-HCV were visualized by EM at low and high magnifications (Fig. 2C to F). In MVA-HCV but not in MVA-WT (data not shown) infected cells, we observed several morphological alterations, such as a loss of spatial organization of the ER, with vesicles embedded in a membrane matrix of circular or tightly undulating membranes, forming electron-dense structures (EDS; Fig. 2C to E), as well as the presence of swollen mitochondria (m; Fig. 2F). A higher magnification of the cytoplasmic dense aggregates revealed membranes and tubular structures (TS) as part of the EDS (Fig. 2D to F).

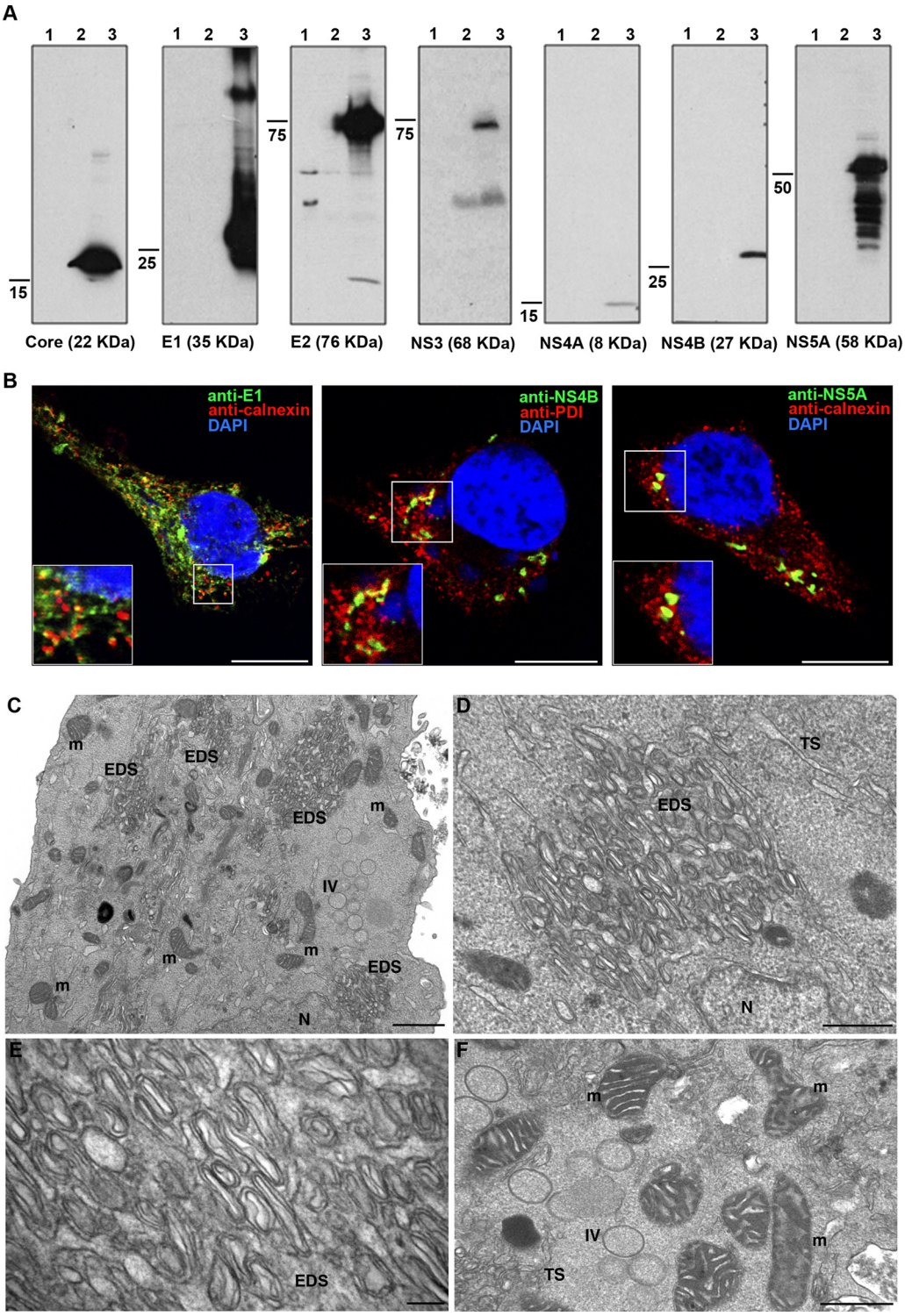

FIG 2 Expression of HCV proteins by MVA-HCV. (A) Expression of HCV proteins by Western blotting with specific antibodies against Core, E1, E2, NS3, NS4A, NS4B, and NS5A proteins. Lanes: 1, mock-infected cells; 2, MVA-WT-infected cells; 3, MVA-HCV-infected cells. (B) Immunofluorescence analysis of HCV proteins produced in HeLa cells infected with MVA-HCV. Subconfluent HeLa cells infected with MVA-HCV were fixed at 16 hpi, labeled with the corresponding primary antibodies, followed by the appropriate fluorescent secondary antibodies and visualized by confocal microscopy. The antibodies used were anti-E1, anti-NS4B, or anti-NS5A to detect HCV proteins, anti-calnexin, or anti-PDI to detect the ER and DAPI to detect DNA. The colocalization is shown at a higher resolution in the boxed area. Bar, 10 μm. (C to F) Architecture of HeLa cells following the expression of HCV proteins from MVA-HCV as observed by electron microscopy. HeLa cells infected with the recombinant MVA-HCV were chemically fixed at 16 hpi and then processed for conventional embedding in an epoxy resin. (C) General overview of cells infected with MVA-HCV showing few immature viruses (IVs), a large electron-dense structure (EDS), and swollen mitochondria (m). Scale bar, 1 μm. (D to F) Higher magnifications of MVA-HCV-infected cells showing EDS with membranes and TS (D and E) and swollen mitochondria (F). N, nucleus; m, mitochondria; IV, immature virus; TS, tubular structures; EDS, electron-dense structures in membranous webs. Scale bars: 500 nm (D and F), 100 nm (E).

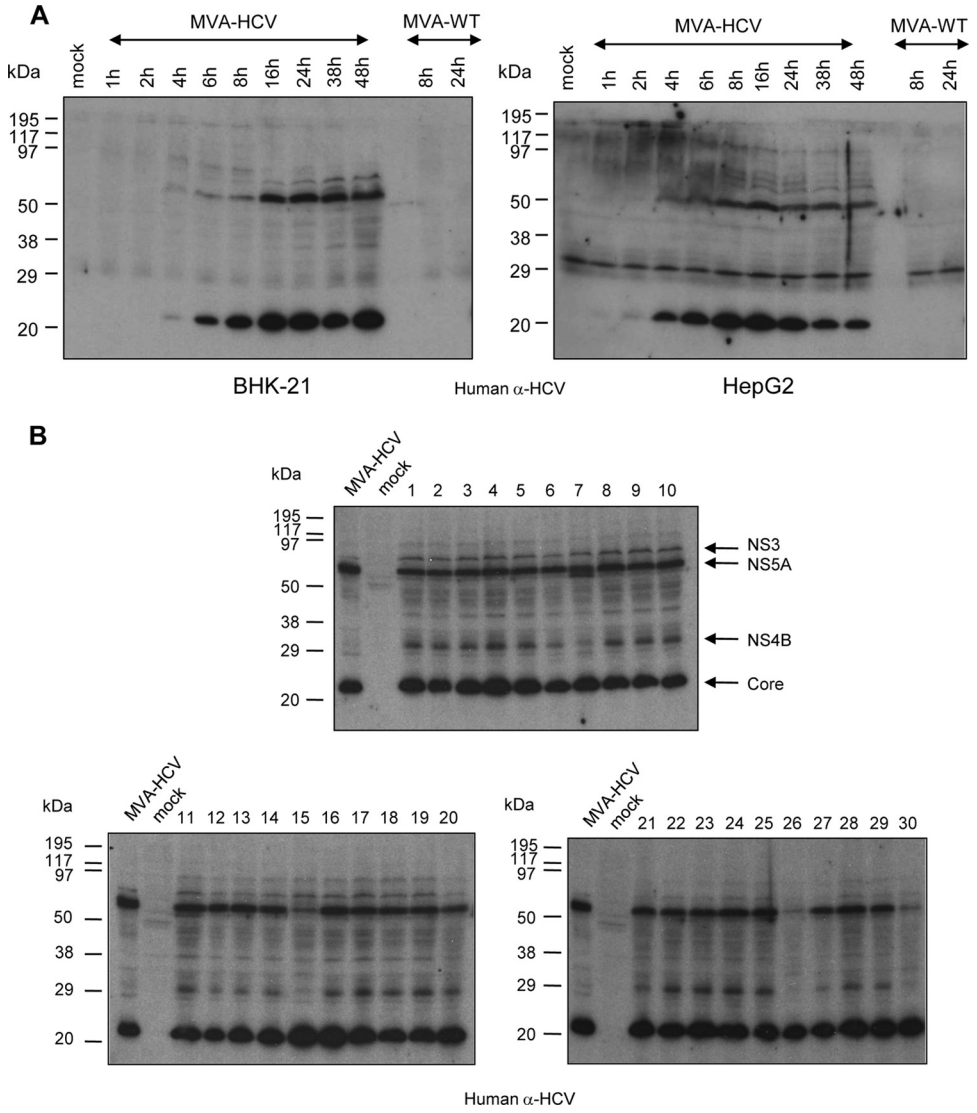

FIG 3 Kinetics of expression and stability of MVA-HCV. (A) Time-course expression of HCV proteins in BHK-21 and HepG2 cells. The expression of HCV proteins at the indicated times postinfection was visualized by Western blotting in samples of mock-infected or infected cells with MVA-WT or MVA-HCV using HCV antibody-positive human sera. (B) Analysis of the stability of the HCV proteins expressed by MVA-HCV. Thirty individual plaques isolated from MVA-HCV-infected cells at passage 11 were grown in BHK-21 cells and lysed, and proteins were fractionated by SDS–12% PAGE and analyzed by Western blotting with an HCV antibody-positive human sera.

Although there was formation of immature virus (IV) forms of MVA (Fig. 2C), no virus-like particles (VLPs) of HCV were detected in infected cells.

(iii) Time-course expression analysis and genetic stability of MVA-HCV. In order to assay the kinetic of HCV protein expression from MVA-HCV, we carried out a time-course analysis in both BHK-21 cells and the hepatic HepG2 cell line. Western blot analyses with a human polyclonal antibody revealed that in BHK-21 and HepG2 cells, HCV polyprotein is processed and detected as early as 2 to 4 hpi (Fig. 3A).

To verify that MVA-HCV recombinant virus can be maintained in cultured cells without the loss of the transgene, a stability test was performed. The recombinant MVA-HCV was continuously grown from passage 7 (P2 stock) to passage 11 (P8→P11) in BHK-21 cells. Expression of HCV proteins at the different passages was determined by Western blotting with a human anti-HCV antibody from an infected patient. We observed that MVA-HCV efficiently expresses the HCV proteins after successive passages (data not shown). Moreover, an extract from cells infected at P11 was used for a new round of plaque purification step in BHK-21 cells. Thirty well-isolated plaques were tested for the expression of HCV proteins. All of them (100%) expressed the HCV proteins (Fig. 3B), indicating that the MVA-HCV recombinant virus is genetically stable.

We assume that the major bands seen in the Western blots probed with anti-HCV immune human sera are Core, NS4B, NS5A, and NS3 based on the size of the bands and also based on a previous study demonstrating that the major immunogenic HCV antigens were Core, NS4B, NS3, and NS5A proteins, which were recognized in 97, 86, 68, and 53% of the patient sera, respectively (36).

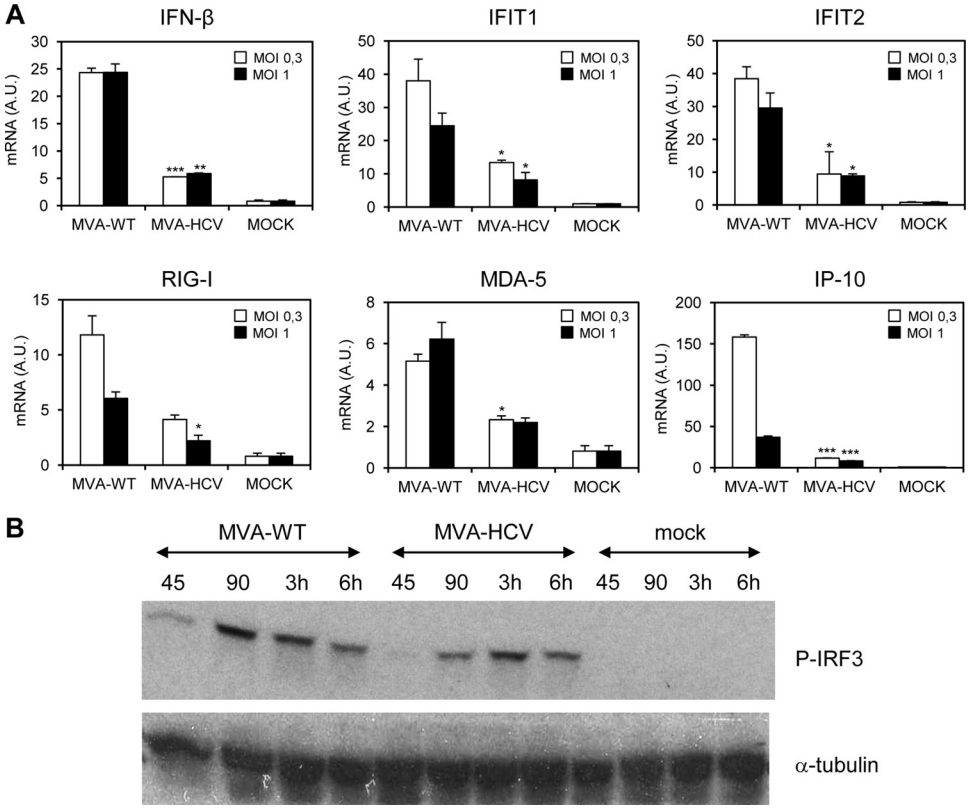

FIG 4 Differential expression of genes involved in innate immunity by MVA-HCV recombinant and parental MVA-WT viruses. (A) Analysis of gene expression by reverse transcription-PCR (RT-PCR). Human monocyte-derived DCs were mock infected or infected with MVA-WT or MVA-HCV at 0.3 or 1 PFU/cell for 6 h. IFN-β, IFIT1, IFIT2, RIG-I, MDA-5, and IP-10 mRNA levels were quantified by RT-PCR. mRNA results are expressed as the ratio of the gene of interest to *Hprt* mRNA levels. AU, arbitrary units. *, $P < 0.05$; **, $P < 0.005$; and ***, $P < 0.001$ for all conditions comparing MVA-HCV to MVA-WT at the same MOI. (B) Induction of IRF-3 phosphorylation by parental MVA-WT and recombinant MVA-HCV viruses in THP-1 cell line. The membrane was also probed with an antibody against cellular α-tubulin as a loading control.

MVA-HCV recombinant and parental MVA-WT viruses differentially express genes involved in innate immunity. Since it is widely accepted that in natural infection some HCV proteins impair the response of innate immune cells to HCV virus, we decided to evaluate the effect of HCV protein expression from MVA-HCV in human DCs compared to the parental MVA-WT. As shown in Fig. 4A, by real-time PCR in DCs infected for 6 h, the expression of beta interferon (IFN-β), IFN-β-induced genes (*IFIT1* and *IFIT2*), and chemokine IP-10 was downregulated compared to the parental virus. To a lesser extent, the expression of the cytosolic RLR pattern recognition receptors RIG-I and MDA-5 was also downregulated in DCs infected with MVA-HCV compared to the parental virus. However, the mRNA levels of these proteins were significantly upregulated by both viruses compared to mock-infected cells.

We also evaluated the expression of some inflammatory cytokines and chemokines in the supernatants of infected DCs by using Luminex. The expression of these proteins was higher in DCs infected with MVA-HCV or MVA-WT than in mock-infected cells, but some differences between both viruses were observed. The levels of IL-1β and IL-6, although low, were comparable in both infections, whereas the amounts of IL-8, MIP-1α, and tumor necrosis factor alpha (TNF-α) change depending of the virus. MVA-HCV induces higher levels of IL-8 and MIP-1α, and MVA-WT induces higher levels of TNF-α (not shown).

In order to confirm previous results, we decided to evaluate the phosphorylation status of IRF-3 protein after infection with the parental or the recombinant viruses in human macrophage cells (THP-1). As shown in Fig. 4B, in contrast to mock-infected cells, both MVA-HCV and MVA-WT induced similar levels of P-IRF3 although the kinetic of expression was somewhat delayed in MVA-HCV infection.

These findings indicate that, as in the natural infection, the expression of HCV proteins from MVA-HCV modulates the expression of genes involved in innate immunity. Nevertheless, since they are expressed in the context of MVA infection, which is known to efficiently induce innate immunity, the overall effect will be a positive activation of immune cells.

MVA-HCV induces high, broad, polyfunctional, and long-lasting HCV-specific T cell immune responses in C57BL/6 mice when used in a homologous or heterologous prime-boost combination. (i) Adaptive immune response. To assay the immunogenicity of MVA-HCV, we analyzed the HCV-specific T cell adaptive immune responses elicited in mice by using homologous (MVA-HCV/MVA-HCV) or heterologous (DNA-HCV/MVA-HCV) prime-boost approaches.

C57BL/6 mice, four in each group, were immunized as described in Materials and Methods. Adaptive T cell immune responses were measured 10 days after the last immunization by a polychromatic ICS assay. Splenocytes from immunized animals

were stimulated *ex vivo* for 6 h with a panel of 457 peptides (13- to 19-mers overlapping by 11 or 12 amino acids) grouped in six pools—Core (28 peptides), E (83 peptides), p7+NS2 (40 peptides), NS3 (98 peptides), NS4 (47 peptides), and NS5 (161 peptides)—and stained with specific antibodies to identify T cell lineage (CD3, CD4, and CD8), degranulation (CD107a), and responding cells (IL-2, IFN-γ, and TNF-α). Animals primed with either nonrecombinant MVA-WT or sham DNA (DNA-ϕ) and boosted with the MVA-WT were used as control groups.

The percentages of T cells producing IFN-γ and/or IL-2 and/or TNF-α established the overall $CD4^+$ T cell responses, whereas the percentages of T cells producing CD107a and/or IFN-γ and/or IL-2 and/or TNF-α determined the overall $CD8^+$ T cell responses. The magnitude of the HCV-specific $CD8^+$ T cell responses, determined as the sum of the individual responses obtained for the Core, E, p7+NS2, NS3, NS4, and NS5 peptide pools, was significantly higher in animals immunized with MVA-HCV/MVA-HCV or DNA-HCV/MVA-HCV protocols compared to their respective control groups, where the antigen-specific responses were very low ($P < 0.005$) (Fig. 5A). In both groups, the vaccine-elicited immune response was mediated by the CD8 T cell subset since no specific $CD4^+$ T cell response was detected (Fig. 5A).

The $CD8^+$ T cell responses were higher in magnitude and significantly higher in mice receiving the heterologous DNA-HCV/MVA-HCV regimen ($P < 0.005$). In animals from MVA-HCV/MVA-HCV group, 90% of the $CD8^+$ T cell responses were directed against the p7+NS2 pool, whereas in animals from DNA-HCV/MVA-HCV group, 97% of the $CD8^+$ T cell responses were directed against the NS3 pool (Fig. 5A and B).

The quality of a T cell response can be characterized in part by the pattern of cytokine production and its cytotoxic potential. On the basis of the analysis of IFN-γ, IL-2, and TNF-α secretion, as well as the study of CD107a expression on the surface of activated T cells as an indirect marker of cytotoxicity, 16 distinct HCV-specific $CD8^+$ T cell populations were identified (Fig. 5C). For each population, the background detected in the nonstimulated control sample was subtracted. The HCV-specific $CD8^+$ T cell responses elicited by both immunization approaches were highly polyfunctional, with >60% of the $CD8^+$ T cells exhibiting two, three, or four functions. The higher magnitude of the antigen-specific response obtained in the DNA-HCV/MVA-HCV group compared to the MVA-HCV/MVA-HCV group was due to an enhancement in the absolute frequencies of the $CD8^+$ T cells producing CD107a, CD107a and TNF-α, or CD107a, IFN-γ, and TNF-α.

(ii) Memory immune response. The durability of a vaccine-induced T cell response is an important feature since long-term protection is a requirement for prophylactic vaccination. Thus, we decided to analyze the phenotype of memory vaccine-induced T cell responses in the spleens and livers of immunized mice at 53 days after the last immunization by using the polychromatic ICS assay. At this time, splenocytes and IHICs isolated from immunized mice were stimulated *ex vivo* for 6 h with the HCV peptide pools and stained with specific antibodies to identify T cell lineage (CD3, CD4, and CD8), degranulation (CD107a), responding cells (IFN-γ, IL-2, and TNF-α) and memory stages (CD127 and CD62L).

In the spleen, the magnitude of the memory HCV-specific $CD4^+$ and $CD8^+$ T cell responses was significantly higher in animals immunized with MVA-HCV/MVA-HCV or DNA-HCV/MVA-HCV immunization protocols compared to their respective control groups, where the antigen-specific responses were very low or absent ($P < 0.005$) (not shown).

As shown in Fig. 6A, in both groups the memory vaccine-elicited immune response was mainly mediated by the CD8 T cell subset. At this time point, low-magnitude memory $CD4^+$ T cell responses were only detected in MVA-HCV/MVA-HCV immunization groups. The $CD4^+$ T cell responses were similarly directed against the Core (47%) and E (53%) peptide pools.

The memory $CD8^+$ T cell responses were higher in magnitude and significantly higher in mice receiving the heterologous DNA-HCV/MVA-HCV regimen ($P < 0.005$). In splenocytes from animals of the MVA-HCV/MVA-HCV group, 91% of the $CD8^+$ T cell responses were directed against the p7+NS2 pool, and the rest of the responses were distributed against the NS3 (7%) and E (2%) pools. In animals from the DNA-HCV/MVA-HCV group, the $CD8^+$ T cell responses were mainly directed against the NS3 (70%) and p7+NS2 (19%) pools, whereas the rest of the responses were distributed against the NS4 (9%) and E (2%) pools (Fig. 6A).

The splenic HCV-specific memory $CD8^+$ T cell responses elicited by both immunization protocols were highly polyfunctional, with >90% of the $CD8^+$ T cells exhibiting two, three, or four functions (Fig. 6B). Vaccine-induced $CD8^+$ T cells predominantly coproduced either CD107a, IFN-γ, and TNF-α or CD107a, IL-2, IFN-γ, and TNF-α.

Since previous studies have shown that CD127 and CD62L define functionally distinct populations of memory antigen-specific T cells (37), we characterized the differentiation stages of the responding $CD8^+$ T cells into central memory (TCM; $CD127^+$ $CD62L^+$), effector memory (TEM; $CD127^+$ $CD62L^-$), or effector (TE; $CD127^-$ $CD62L^-$) populations. In both immunization groups, 70% of the HCV-specific $CD8^+$ T cells were of the TEM phenotype (Fig. 6C).

Next, we characterized the memory vaccine-induced T cell immune responses in the liver. Since the yields of IHIC isolation were low, we decided to analyze the hepatic memory HCV-specific immune responses using only four stimuli: p7+NS2, NS3, a mix (Core+E+NS4+NS5), and RPMI.

The pattern of the vaccine-induced T cell memory response in the liver was very similar to that obtained in the spleen. In both groups, the memory HCV-specific immune response was mainly mediated by the CD8 T cell subset. The memory $CD4^+$ T cell responses were low in magnitude and only detected in the DNA-HCV/MVA-HCV immunization group. The $CD4^+$ T cells were directed against the mix (66%) and p7+NS2 (34%) pools. The memory $CD8^+$ T cell responses were higher in magnitude, although in this case the frequencies of the $CD8^+$ T cells producing cytokines were similar in both groups. Again, the $CD8^+$ T cell responses in animals from MVA-HCV/MVA-HCV group were mainly directed against the p7+NS2 (97%) pool, while in animals from DNA-HCV/MVA-HCV group the $CD8^+$ T cell responses were largely directed against the NS3 (72%) and p7+NS2 (24%) pools (Fig. 7A).

The HCV-specific memory $CD8^+$ T cell responses induced by both immunization protocols in the liver were highly polyfunctional, with >80% of the $CD8^+$ T cells exhibiting two, three, or four functions (Fig. 7B). Vaccine-induced $CD8^+$ T cells mainly coproduced CD107a, IFN-γ, and TNF-α and were predominantly of the TEM phenotype (Fig. 7C).

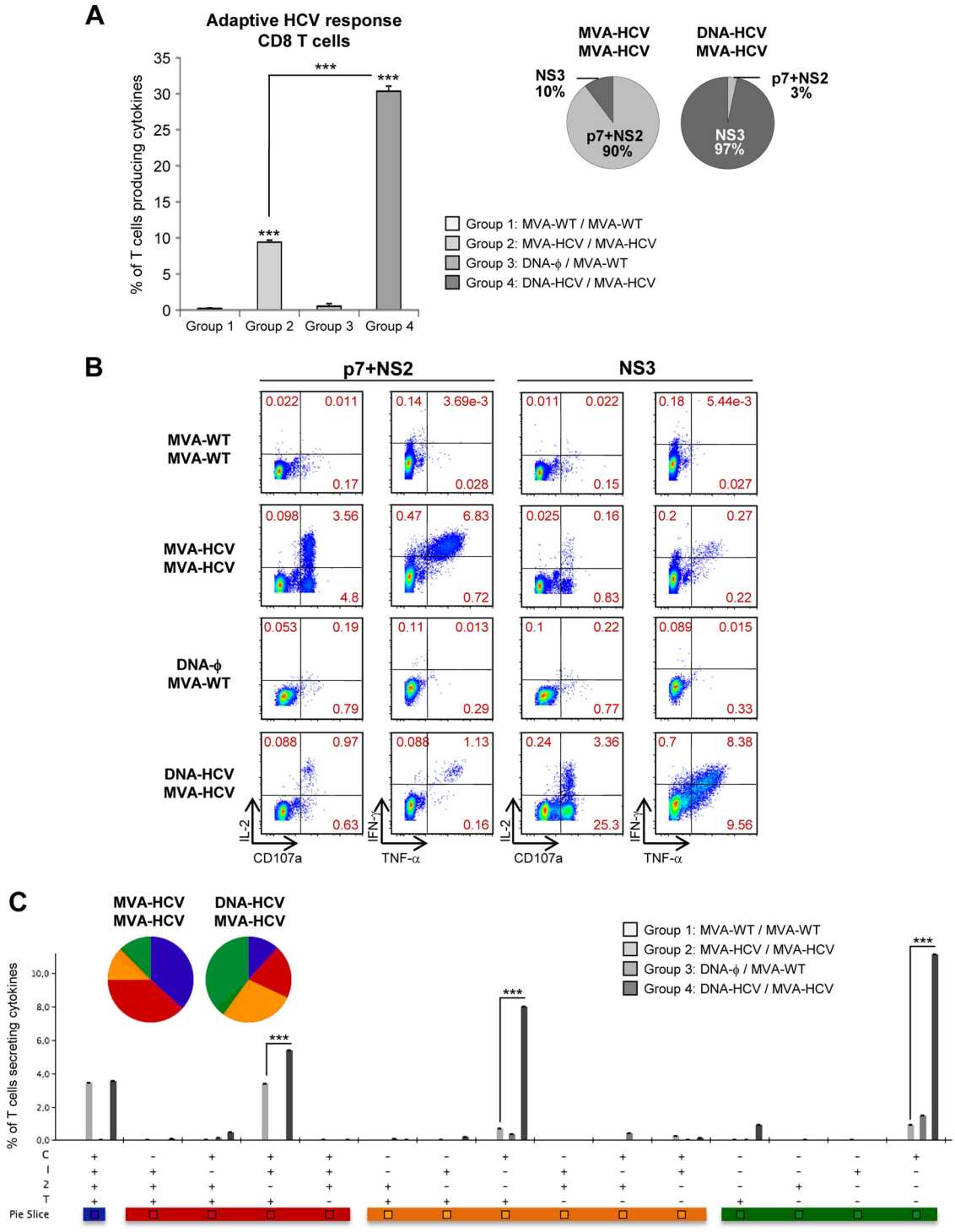

FIG 5 Adaptive HCV-specific T cell immune responses elicited by MVA-HCV recombinant virus in the spleen of C57BL/6 mice in homologous or heterologous immunization protocols. (A) Magnitude of the vaccine-specific $CD8^+$ T cell response. The HCV-specific $CD8^+$ T cells were measured 10 days after the last immunization by ICS assay after stimulation of splenocytes derived from immunized animals with the different HCV peptide pools. The total value in each group represents the sum of the percentages of $CD8^+$ T cells secreting CD107a and/or IFN-γ and/or IL-2 and/or TNF-α against all HCV peptide pools. The right diagrams represent the contribution of specific HCV peptide pools to the total $CD8^+$ T cell response in the different immunization groups. All data are background subtracted. ***, $P < 0.001$. The *P* value indicates significantly higher responses compared to parental groups or between DNA-HCV/MVA-HCV and MVA-HCV/MVA-HCV immunization groups. (B) Flow cytometry profiles of vaccine-induced $CD8^+$ T cell responses against the p7+NS2 or NS3 peptide pools. (C) Functional profile of the adaptive HCV-specific $CD8^+$ T cell response in the different immunization groups. All of the possible combinations of the responses are shown on the *x* axis, whereas the percentages of the functionally distinct cell populations within the total CD8 T cell population are shown on the *y* axis. Rows: C, CD107a; I, IFN-γ; 2, IL-2; T, TNF-α. Responses are grouped and color-coded on the basis of the number of functions. ***, $P < 0.001$.

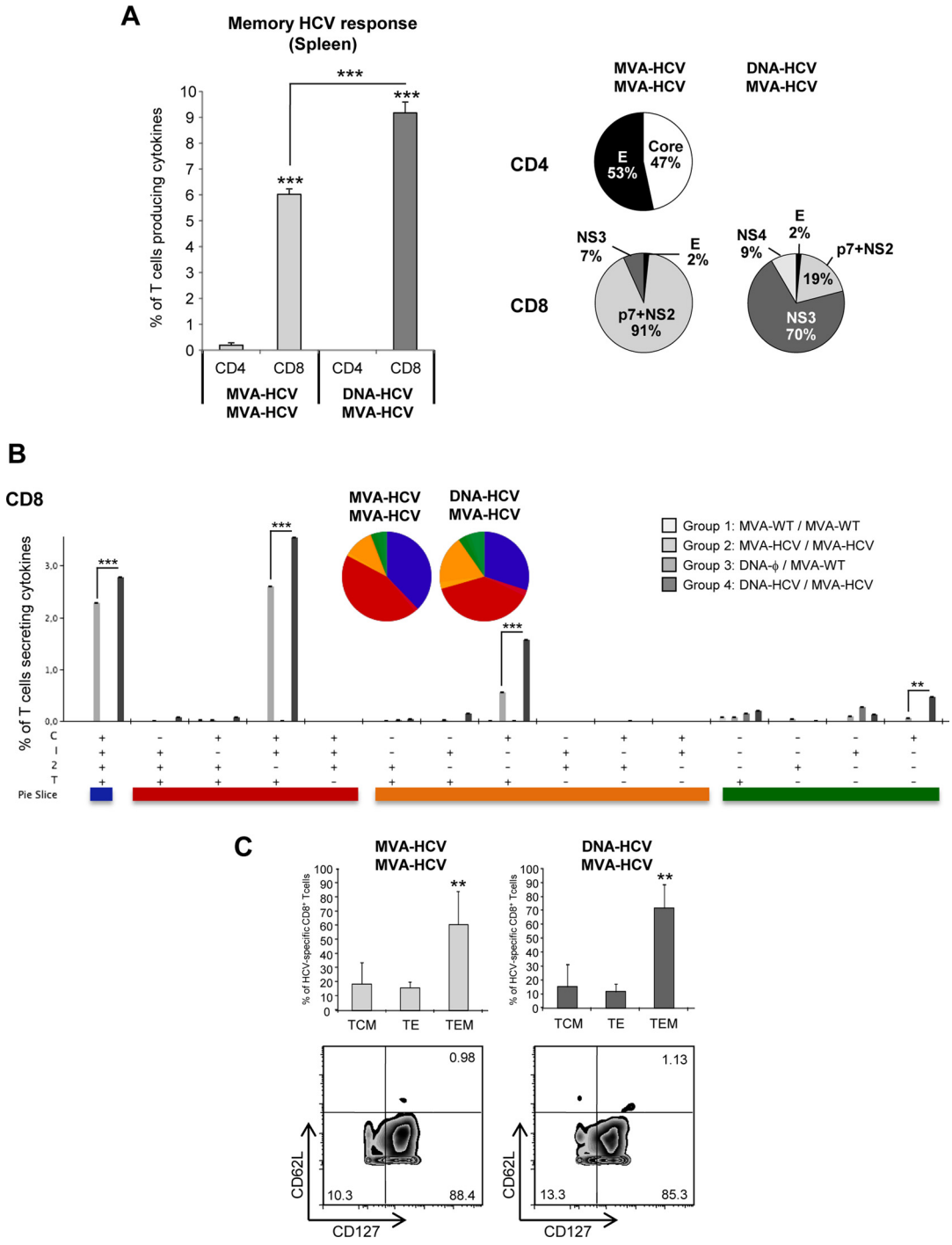

FIG 6 Memory HCV-specific T cell immune responses elicited by MVA-HCV recombinant virus in the spleen of C57BL/6 mice in homologous or heterologous immunization protocols. (A) Magnitude of the vaccine-specific $CD4^+$ or $CD8^+$ T cell responses. The HCV-specific $CD4^+$ or $CD8^+$ T cells were measured in the spleen 53 days after the last immunization by ICS assay after stimulation of splenocytes derived from immunized animals with different HCV peptide pools. The total value in each group represents the sum of the percentages of $CD4^+$ or $CD8^+$ T cells secreting IFN-γ and/or IL-2 and/or TNF-α (CD4) or CD107a and/or IFN-γ and/or IL-2 and/or TNF-α (CD8) against all HCV peptide pools. The right diagrams represent the contribution of specific HCV peptide pools to the total $CD4^+$ or $CD8^+$ T cell responses in the different immunization groups. All data are background subtracted. ***, $P < 0.001$. The *P* value indicates significantly higher responses compared to $CD4^+$ T cell responses or between $CD8^+$ T cell responses obtained in DNA-HCV/MVA-HCV compared to MVA-HCV/MVA-HCV immunization groups. (B) Functional profile of the memory HCV-specific $CD8^+$ T cell response in the different immunization groups. All of the possible combinations of the responses are shown on the *x* axis, whereas the percentages of the functionally distinct cell populations within the total $CD8^+$ T cell population are shown on the *y* axis. Rows: C, CD107a; I, IFN-γ; 2, IL-2; T, TNF-α. Responses are grouped and color-coded on the basis of the number of functions. **, $P < 0.005$; ***, $P < 0.001$. (C) Phenotypic profile of memory HCV-specific $CD8^+$ T cells. Upper graphics represent the percentage of total HCV-specific $CD8^+$ T cells with central memory (TCM; $CD127^+$ $CD62L^+$), effector memory (TEM; $CD127^+$ $CD62L^-$), or effector (TE; $CD127^-$ $CD62L^-$) phenotype. Lower diagrams correspond to representative fluorescence-activated cell sorting (FACS) plots showing the percentage of p7+NS2 (left) or NS3 (right)-specific CD8 T cells with central memory, effector memory, or effector phenotype. **, $P < 0.005$.

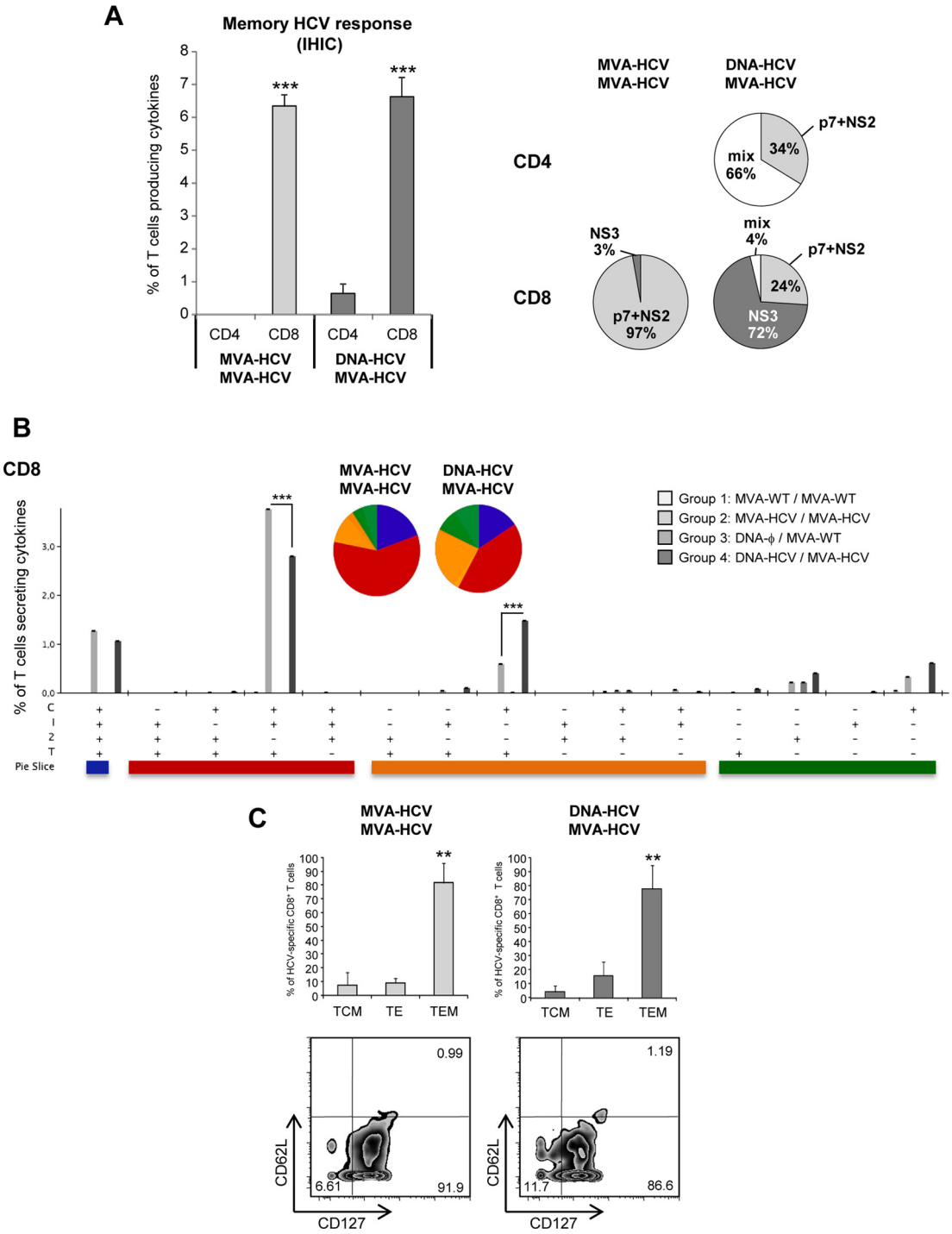

FIG 7 Memory HCV-specific T cell immune responses elicited by MVA-HCV recombinant virus in the liver of C57BL/6 mice in homologous or heterologous immunization protocols. (A) Magnitude of the vaccine-specific $CD4^+$ or $CD8^+$ T cell responses. The HCV-specific $CD4^+$ or $CD8^+$ T cells were measured in the liver 53 days after the last immunization by ICS assay after stimulation of IHICs isolated from immunized animals with the different HCV peptide pools. The total value in each group represents the sum of the percentages of $CD4^+$ or $CD8^+$ T cells secreting IFN-γ and/or IL-2 and/or TNF-α (CD4) or CD107a and/or IFN-γ and/or IL-2 and/or TNF-α (CD8) against all HCV peptide pools. The right diagrams represent the contribution of specific HCV peptide pools to the total $CD4^+$ or $CD8^+$ T cell responses in the different immunization groups. All data are background subtracted. ***, $P < 0.001$. The *P* value indicates significantly higher responses compared to $CD4^+$ T cell responses in the different immunization groups. (B) Functional profile of the memory HCV-specific $CD8^+$ T cell response in the different immunization groups. All of the possible combinations of the responses are shown on the *x* axis, whereas the percentages of the functionally distinct cell populations within the total $CD8^+$ T cell population are shown on the *y* axis. Rows: C, CD107a; I, IFN-γ; 2, IL-2; T, TNF-α. Responses are grouped and color coded on the basis of the number of functions. ***, $P < 0.001$. (C) Phenotypic profile of memory HCV-specific $CD8^+$ T cells. The upper graphics represent the percentage of total HCV-specific $CD8^+$ T cells with central memory (TCM; $CD127^+$ $CD62L^+$), effector memory (TEM; $CD127^+$ $CD62L^-$), or effector (TE; $CD127^-$ $CD62L^-$) phenotype. Lower diagrams correspond to representative FACS plots showing the percentage of p7+NS2 (left)- or NS3 (right)-specific CD8 T cells with central memory, effector memory or effector phenotype. **, $P < 0.005$.

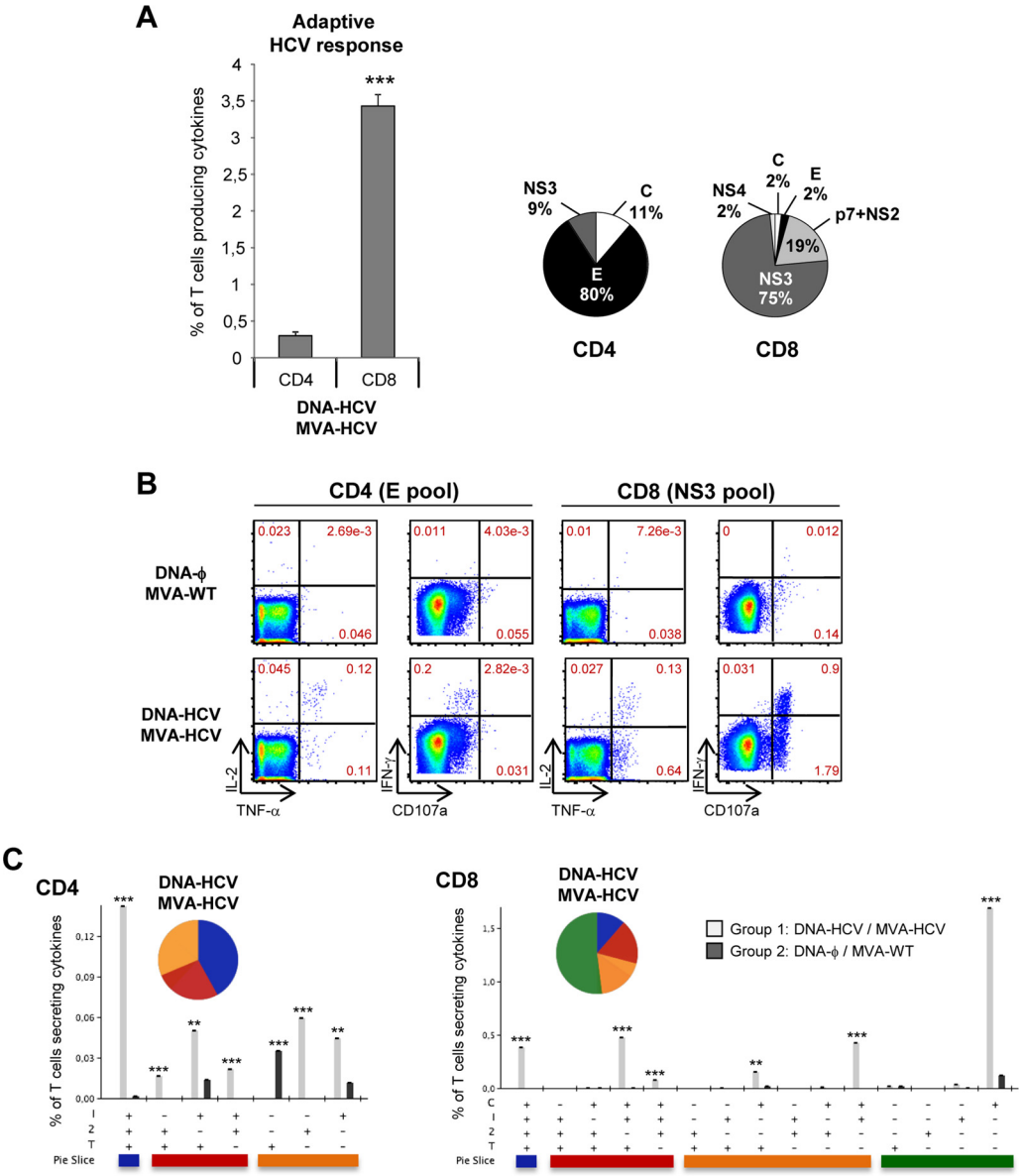

FIG 8 Adaptive HCV-specific T cell immune responses elicited by MVA-HCV recombinant virus in the spleen of HLA-A2 transgenic mice in a heterologous immunization protocol. (A) Magnitude of the vaccine-specific $CD4^+$ or $CD8^+$ T cell responses. The HCV-specific $CD4^+$ or $CD8^+$ T cells were measured 10 days after the last immunization by ICS assay after stimulation of splenocytes derived from immunized animals with the different HCV peptide pools. The total value in each group represents the sum of the percentages of $CD4^+$ or $CD8^+$ T cells secreting IFN-γ and/or IL-2 and/or TNF-α (CD4) or CD107a and/or IFN-γ and/or IL-2 and/or TNF-α (CD8) against all HCV peptide pools. The right diagrams represent the contribution of specific HCV peptide pools to the total $CD4^+$ or $CD8^+$ T cell response. All data are background subtracted. ***, $P < 0.001$. The *P* value indicates significantly higher response compared to CD4 T cell response. (B) Flow cytometry profiles of vaccine-induced CD4 or CD8 T cell responses against the E (CD4) or NS3 (CD8) peptide pools. (C) Functional profile of the adaptive HCV-specific $CD4^+$ or $CD8^+$ T cell responses in the different immunization groups. All of the possible combinations of the responses are shown on the *x* axis, whereas the percentages of the functionally distinct cell populations within the total $CD4^+$ or $CD8^+$ T cell populations are shown on the *y* axis. Rows: C, CD107a; I, IFN-γ; 2, IL-2; T, TNF-α. Responses are grouped and color coded on the basis of the number of functions. **, $P < 0.005$; ***, $P < 0.001$.

High polyfunctional and sustained HCV-specific T cell immune responses elicited in HLA-A2 transgenic mice receiving heterologous DNA-HCV/MVA-HCV protocol. Since in previous analysis the heterologous DNA-HCV/MVA-HCV protocol elicited the highest magnitude of HCV-specific response in the C57BL/6 mouse model, we decided to evaluate the same approach but in the HLA-A2 transgenic mice. These transgenic mice express a chimeric form of HLA-A2.1 and have previously been shown to elicit a repertoire of HCV-specific responses similar to that seen in the infected human population (38).

At 10 days after the boost, the adaptive T cell immune response was assayed in splenocytes from immunized animals stimulated *ex vivo* for 6 h with different HCV peptide pools as previously described. Mice primed with sham DNA (DNA-ϕ) and boosted with the MVA-WT were used as a control group.

As in the C57BL/6 mice, the vaccine-elicited adaptive immune

response was mainly mediated by the CD8 T cell subset (Fig. 8A). $CD4^+$ T cell responses were low in magnitude, although directed against multiple HCV pools, with the E (80%) and Core (11%) pools being the most recognized. $CD8^+$ T cell responses showed the highest magnitude and were mostly directed against the NS3 (75%) and p7+NS2 (19%) pools (Fig. 8A and B). Both $CD4^+$ and $CD8^+$ antigen-specific T cells were highly polyfunctional, with >50% of the cells exhibiting two, three, or four functions (Fig. 8C). The $CD4^+$ T cells predominantly coproduced IFN-γ, IL-2, and TNF-α, whereas the $CD8^+$ T cells showed an enhanced cytotoxic profile, represented by an activated T cell population expressing a high frequency of CD107a on their surfaces.

The memory T cell immune response was assayed at 53 days after the boost. The HCV-specific response was elicited only by the $CD8^+$ T cells and mainly directed against the p7+NS2 (72%) and NS3 (28%) pools (Fig. 9A and B). As in the adaptive phase, the memory HCV-specific $CD8^+$ T cells were highly polyfunctional, with a high frequency of cells expressing simultaneously CD107a, IFN-γ, IL-2, and TNF-α (Fig. 9C) and with TEM (54% ± 3%) and TCM (34% ± 5%) phenotypes (Fig. 9D).

DISCUSSION

Over the last decade diverse HCV vaccine candidates have been explored in mice and primates. However, only a small number of them have progressed to human clinical trials. Most of these trials have assessed potential therapeutic vaccine candidates in HCV-infected patients. A smaller number have evaluated candidates in healthy volunteers with the aim of developing a prophylactic HCV vaccine or to serve as a bridge to evaluate vaccines in HCV-infected patients. Four main vaccine approaches have been explored in human clinical trials: recombinant proteins, peptides, DNA, and viral vectors (6, 18, 19). Among them, the viral vector-based vaccines using the poxvirus platform have been shown to be highly immunogenic with promising results. In this investigation, we described the immune characteristics of a new poxvirus vaccine candidate MVA-HCV that highlights its potential as a T cell immunogen.

Poxviruses offer attractive and unique properties for the generation of highly stable recombinant vectors as vaccine candidates; hence, they are increasingly used in the prevention and treatment of emergent infectious diseases and cancer, in particular, those candidates based on the highly attenuated ALVAC, MVA, and NYVAC strains (39, 40). Here we have successfully generated a stable MVA recombinant that constitutively expresses all of the HCV structural and nonstructural (except for 390 amino acids from the C-terminal part of NS5B) proteins from genotype 1a. We decided to include the nearly full-length genome in order to target almost all of the T and B cell determinants described for HCV and for safety considerations. It has been previously reported that a narrow monospecific $CD8^+$ T cell response was associated with persistent viremia and poor disease outcome (41). This reinforces the importance of targeting multiple $CD8^+$ T cell epitopes by vaccination to ensure a broad response available to compensate for any losses in $CD8^+$ T cell subpopulations due to epitope escape.

This is the first time in which all of the HCV proteins are expressed in the same context by a single virus vector. Usually, the HCV vaccine candidates target the structural proteins (Core, E1, and E2) (42–45), a combination of structural and nonstructural proteins (Core, NS3, and NS4) (46–48), or the nonstructural proteins (generally NS3, NS4, and NS5) (20, 25). Undoubtedly, the most frequently used HCV antigen is NS3 since the majority of the viral epitopes recognized by cytotoxic T lymphocytes and $CD4^+$ T cells in patients with HCV infection are located in this protein (9, 49).

Expression of HCV proteins from MVA-HCV triggers the cytoplasmic accumulation of dense structures, as visualized by confocal and electron microscopy. These structures are formed by membranes derived from the ER since the HCV proteins E1, NS4B, and NS5A colocalize with ER markers. The membranous web is believed to be the local HCV replication site, although in MVA-HCV infection there is no production of VLPs but the formation of membrane aggregates placed at different sites in the cell cytoplasm. This membrane accumulation is more prevalent than during WR-HCV infection (30), probably as a result of reduced cell killing mediated by MVA versus WR.

It is known that the major strategy used by HCV to subvert the host innate immune response is to undermine IFN antiviral activity, as well as functions of innate immune cells. Regarding the IFN activity, the main targets of HCV are represented by the PAMP signaling pathways, leading to IRF-3 activation, the IFN-α/β receptor signaling pathway, and the ISG effector proteins. In this inhibition are involved the HCV proteins NS3/4A, Core, NS5A, and E2 (50). Although we have shown that the expression of HCV proteins in MVA-HCV-infected human monocyte-derived DCs affects mRNA levels, the expression of IFN-β, some IFN-β-induced genes, chemokines, and to a lesser extent the cytosolic RLR pattern recognition receptors compared to the parental MVA-WT, the overall effect observed was an upregulation of such genes compared to mock-infected cells. This was confirmed when we analyzed the phosphorylation status of IRF-3 in THP-1 cells where, in contrast to mock-infected cells, both MVA-HCV and MVA-WT induced similar levels of P-IRF3, although the kinetics of expression were somewhat delayed in MVA-HCV infection. These findings indicate that although the expression of HCV proteins from MVA-HCV modulates the expression of genes that play key roles in the sensing and activation of innate immune responses, since they are expressed in the context of MVA infection, the overall effect is a positive activation of immune cells as the vector MVA enhances *per se* innate immune responses. Hence, the vector effect overtakes impairment of innate immune responses by HCV proteins when delivered by MVA-HCV as live vaccine candidate.

It has been shown that HCV-specific T cell responses play a crucial role in determining the outcome of primary HCV infection and suggested that the control of hepatitis C infection requires early and multispecific class I-restricted $CD8^+$ T cell (9, 51, 52) and class II-restricted $CD4^+$ T cell (53, 54) responses to both structural and nonstructural HCV proteins. Clearance of HCV and protection from reinfection is determined not only by the magnitude and/or breadth of multifunctional $CD8^+$ T cells but also by the quality, functional potency, and cytotoxic potential of HCV-specific $CD8^+$ T cells (55) and the selection of high-avidity $CD8^+$ T cells (56), which respond to a diverse array of HLA-class I-restricted HCV-Core, E1, NS3, NS4, and NS5 epitopes (9, 49, 55).

Here we have demonstrated that MVA-HCV, when delivered in homologous or heterologous prime-boost approaches, was able to stimulate a broad HCV-specific $CD4^+$ and $CD8^+$ T cells against peptide pools representing all of the HCV antigens expressed by

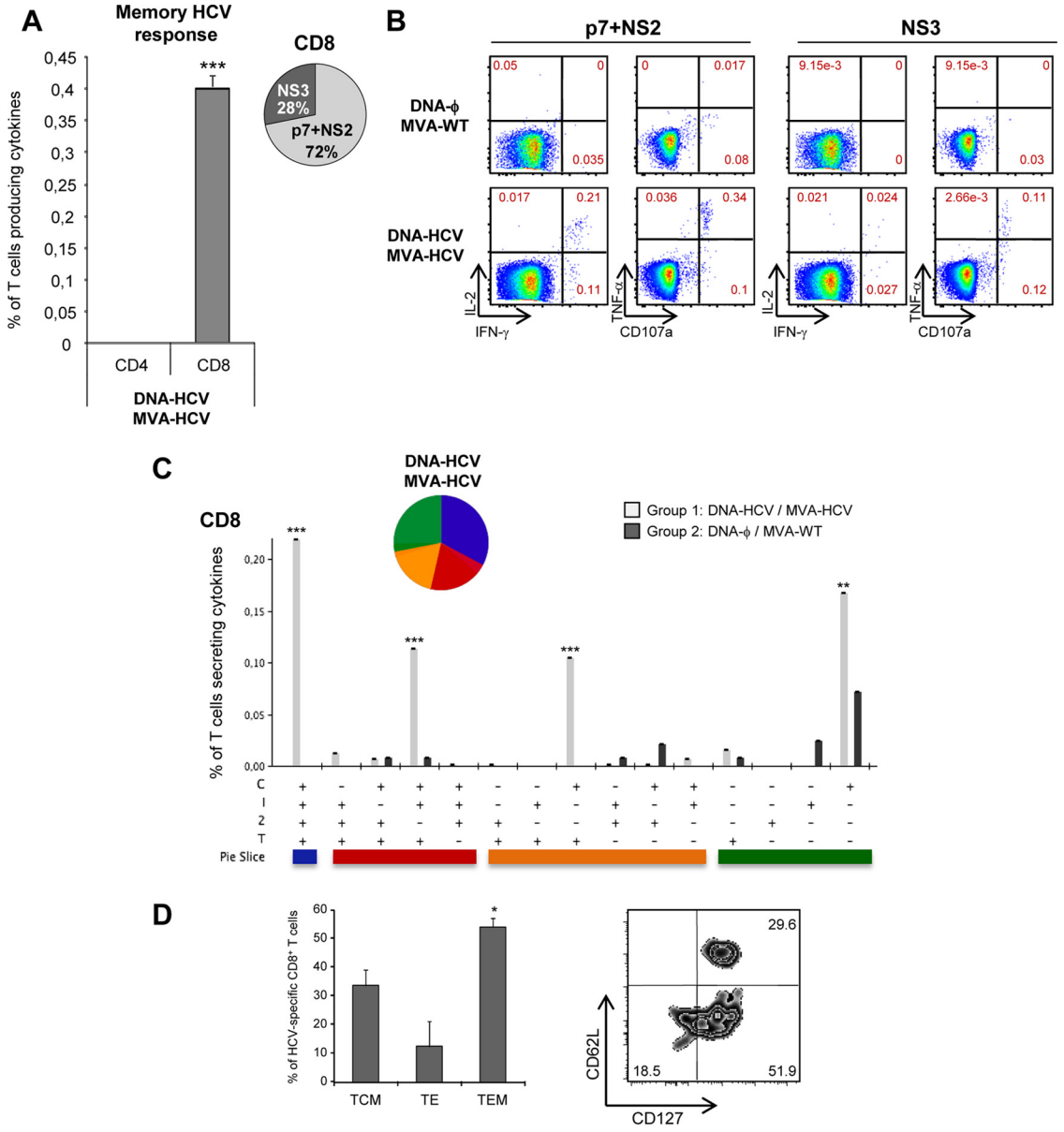

FIG 9 Memory HCV-specific T cell immune responses elicited by MVA-HCV recombinant virus in the spleen of HLA-A2 transgenic mice in heterologous immunization protocol. (A) Magnitude of the vaccine-specific $CD4^+$ or $CD8^+$ T cell responses. The HCV-specific $CD4^+$ or $CD8^+$ T cells were measured 53 days after the last immunization by ICS assay after stimulation of splenocytes derived from immunized animals with the different HCV peptide pools. The total value in each group represents the sum of the percentages of $CD4^+$ or $CD8^+$ T cells secreting IFN-γ and/or IL-2 and/or TNF-α (CD4) or CD107a and/or IFN-γ and/or IL-2 and/or TNF-α (CD8) against all HCV peptide pools. The right diagram represents the contribution of specific HCV peptide pools to the total $CD8^+$ T cell response. All data are background subtracted. ***, $P < 0.001$. The P value indicates significantly higher response compared to CD4 T cell response. (B) Flow cytometry profiles of vaccine-induced $CD8^+$ T cell responses against the p7+NS2 or NS3 peptide pools. (C) Functional profile of the memory HCV-specific CD8 T cell response in the different immunization groups. All of the possible combinations of the responses are shown on the x axis, whereas the percentages of the functionally distinct cell populations within the total $CD8^+$ T cell population are shown on the y axis. Rows: C, CD107a; I, IFN-γ; 2, IL-2; T, TNF-α. Responses are grouped and color coded on the basis of the number of functions. **, $P < 0.005$; ***, $P < 0.001$. (D) Phenotypic profile of memory HCV-specific $CD8^+$ T cells. The left graphic represents the percentage of total HCV-specific $CD8^+$ T cells with a central memory (TCM; $CD127^+$ $CD62L^+$), effector memory (TEM; $CD127^+$ $CD62L^-$), or effector (TE; $CD127^-$ $CD62L^-$) phenotype. The right diagram corresponds to a representative FACS plot showing the percentage of p7+NS2-specific CD8 T cells with a central memory, effector memory, or effector phenotype. *, $P < 0.05$.

MVA-HCV but from genotype 1b. The amino acid sequence homology between HCV 1a and 1b genotypes is not equally distributed throughout the genome. The most conserved antigen is the Core protein (97.4%), followed by NS3-NS4-NS5B (87 to 92%) and E1-E2-p7 (81%), and the least conserved antigens are NS2 and NS5A (78%). However, even in regions with reduced homology, the interpretation of the data regarding the contribution of specific peptide pools to the total $CD4^+$ and $CD8^+$ T cell responses should not be very different. A comparative vaccine study performed by Himoudi et al. in HLA-A2.1 transgenic mice revealed that the three antigens containing the most highly immunogenic epitopes are E2, NS3, and NS5B, followed by NS4B and

Core. Overall, E1 and NS5A appear as very weak immunogens. When they performed alignments of these epitopes with existing genotypes 1b, 1a, and 4 sequences present in the database, they observed that some of the highest percentages of conservation were found, not only in the expected highly conserved Core antigen but also in NS3, E2, NS4, and NS5B. For most peptides, major diverging amino acids were not anchor amino acid residues typically found at positions 2 and 8 (38), demonstrating that a number of these nonvariable, highly conserved epitopes, can be highly immunogenic and dominant in different vaccine contexts.

The overall vaccine-induced T cell response observed in our study was mainly mediated by the CD8 T cell subset; however, although lower in magnitude, the $CD4^+$ T cells were highly polyfunctional and play a determinant role in the maintenance and expansion of high-quality antigen-specific $CD8^+$ T cell populations in spleen. Similar responses were detected using IHICs, suggesting that peripheral immunization was able to result in a large pool of vaccine-specific T cells within the liver.

In a homologous immunization protocol (MVA-HCV/MVA-HCV) the main $CD8^+$ T cell target was the p7+NS2 pool, whereas in a heterologous combination (DNA-HCV/MVA-HCV) the main target was the NS3 pool, although the p7+NS2 pool was also recognized with high frequency. These findings indicate that HCV p7 and NS2 proteins contain immunodominant epitopes that elicit an efficient T cell-specific immune response even when they are expressed in the context of MVA infection, where many immunodominant viral peptides are produced. NS3-specific T cell responses have been linked to viral clearance (9, 49); however, since p7 and NS2 proteins were not previously included in the vaccine candidates, no antigen-specific responses against them have been observed. It was recently reported that the concerted action of p7 and NS2 proteins regulates Core localization at the ER and virus assembly (57). It will be of interest to evaluate to what extent the $CD8^+$ T cell response against p7 and NS2 proteins is relevant in the prevention or even in the onset of viral clearance, as well as their possible use as target antigens for future vaccines.

In addition to p7+NS2 and NS3 antigenic responses, we also detected immune responses to other HCV antigens, such as Core, E1+E2, and NS4. The use of a heterologous DNA-HCV/MVA-HCV immunization regimen induced broader responses compared to the homologous MVA-HCV/MVA-HCV despite the fact that in DNA priming we only included HCV Core, E1, E2, and NS3 antigens. This might be explained by the competence between the epitopes generated by both type of vectors. During DNA priming, the response is only focused on epitopes generated from the processing of the HCV antigens, whereas during MVA-HCV priming not only are HCV epitopes presented but also the vector epitopes. After the virus boost, the few HCV-specific clones activated during the DNA priming are efficiently expanded in addition to the new responses derived from the recombinant virus, but in the MVA-HCV primed animals only the immunodominant HCV responses are expanded. It was previously shown that when two different type of vectors are used to express antigenic sequences designed to allow presentation of a maximum number of epitopes (such as Core-E1-E2), a potent immune response can be observed simultaneously directed against multiple epitopes, including epitopes that are otherwise subdominant in the context of single-vector vaccinations (38). In this case, the dominance of epitopes tends to "even out" in a prime-boost vaccination context compared to single-vectored vaccine regimens.

Although in the present study we have not obtained T cell responses to NS5A antigen, this is not surprising since it has been observed that in HLA-A2.1 transgenic mice the NS5A protein appears as a very weak immunogen (38).

Due to the difficulty in measuring perforin expression in activated $CD8^+$ T cells directly *ex vivo*, we assessed the exposure of CD107a on the surface of activated antigen-specific $CD8^+$ T cells as a surrogate marker for induction of killing. The expression of CD107a was analyzed simultaneously with the secretion of IFN-γ, IL-2, and TNF-α in order to determine the quality and polyfunctionality of vaccine-induced T cell responses. When we analyzed the distribution of polyfunctional T cells in the vaccine-induced population, we found that the majority of the MVA-HCV-induced $CD8^+$ T cells were triple or quadruple cytokine producers.

The memory MVA-HCV-induced $CD8^+$ T cells have a TEM phenotype. TEM cells have been described to stably produce perforin and granzyme B, molecules required to lyse virus-infected cells (58). Of note, HCV-specific TEM cells predominate in patients with an acute HCV infection, whereas TCM cells predominate in patients with a chronic HCV infection (19).

Considering the consensus that for an ideal HCV vaccine to be effective it should aim to trigger specific T cell immune responses with an immunogenic profile of a high frequency of polyfunctional CD4 and CD8 T cells targeting multiple HCV proteins and durable, the immunogenic characteristics of MVA-HCV described here fulfill these criteria.

Until a direct HCV or hepatic challenge model is made available for protective studies in immunocompetent mice, we cannot predict the outcome of the MVA-HCV-induced response in the prevention or treatment of HCV infection. However, our data indicate that MVA-HCV can induce sustained T cell responses of a magnitude and quality associated with protective immunity and open the way for future clinical studies of the MVA-HCV candidate as a prophylactic and/or therapeutic vaccine against HCV.

ACKNOWLEDGMENTS

This investigation was supported by Spanish grant SAF2008-02036 and in part by EU. We are grateful to the NIH Reference Reagent Program for the HCV peptides to subtype 1b. J.G.-A. was supported by a contract from the Ministry of Economy and Competitiveness of Spain.

We are grateful to Charlie Rice (Rockefeller University) for providing the plasmid vector containing the full-length HCV genome from isolate H77 (genotype 1a) and to Ilkka Julkunen (Finland) for the generous gift of plasmid vectors and antibodies to HCV. We especially thank Victoria Jimenez for excellent technical assistance with the preparation of cells and viruses.

REFERENCES

1. **Shepard CW, Finelli L, Alter MJ.** 2005. Global epidemiology of hepatitis C virus infection. Lancet Infect. Dis. **5**:558–567.
2. **Afdhal NH.** 2004. The natural history of hepatitis C. Semin. Liver Dis. **24**(Suppl 2):3–8.
3. **Lauer GM, Walker BD.** 2001. Hepatitis C virus infection. N. Engl. J. Med. **345**:41–52.
4. **Grieve R, Roberts J, Wright M, Sweeting M, DeAngelis D, Rosenberg W, Bassendine M, Main J, Thomas H.** 2006. Cost effectiveness of interferon alpha or peginterferon alpha with ribavirin for histologically mild chronic hepatitis C. Gut **55**:1332–1338.
5. **Pawlotsky JM.** 2012. New antiviral agents for hepatitis C. F1000 Biol. Rep. **4**:5.
6. **Torresi J, Johnson D, Wedemeyer H.** 2011. Progress in the development of preventive and therapeutic vaccines for hepatitis C virus. J. Hepatol. **54**:1273–1285.

7. **Diepolder HM, Zachoval R, Hoffmann RM, Wierenga EA, Santantonio T, Jung MC, Eichenlaub D, Pape GR.** 1995. Possible mechanism involving T-lymphocyte response to nonstructural protein 3 in viral clearance in acute hepatitis C virus infection. Lancet **346**:1006–1007.
8. **Schulze zur Wiesch J, Lauer GM, Day CL, Kim AY, Ouchi K, Duncan JE, Wurcel AG, Timm J, Jones AM, Mothe B, Allen TM, McGovern B, Lewis-Ximenez L, Sidney J, Sette A, Chung RT, Walker BD.** 2005. Broad repertoire of the $CD4^+$ Th cell response in spontaneously controlled hepatitis C virus infection includes dominant and highly promiscuous epitopes. J. Immunol. **175**:3603–3613.
9. **Thimme R, Oldach D, Chang KM, Steiger C, Ray SC, Chisari FV.** 2001. Determinants of viral clearance and persistence during acute hepatitis C virus infection. J. Exp. Med. **194**:1395–1406.
10. **McKiernan SM, Hagan R, Curry M, McDonald GS, Kelly A, Nolan N, Walsh A, Hegarty J, Lawlor E, Kelleher D.** 2004. Distinct MHC class I and II alleles are associated with hepatitis C viral clearance, originating from a single source. Hepatology **40**:108–114.
11. **Shoukry NH, Grakoui A, Houghton M, Chien DY, Ghrayeb J, Reimann KA, Walker CM.** 2003. Memory $CD8^+$ T cells are required for protection from persistent hepatitis C virus infection. J. Exp. Med. **197**:1645–1655.
12. **Semmo N, Lucas M, Krashias G, Lauer G, Chapel H, Klenerman P.** 2006. Maintenance of HCV-specific T-cell responses in antibody-deficient patients a decade after early therapy. Blood **107**:4570–4571.
13. **Yu MY, Bartosch B, Zhang P, Guo ZP, Renzi PM, Shen LM, Granier C, Feinstone SM, Cosset FL, Purcell RH.** 2004. Neutralizing antibodies to hepatitis C virus (HCV) in immune globulins derived from anti-HCV-positive plasma. Proc. Natl. Acad. Sci. U. S. A. **101**:7705–7710.
14. **Pestka JM, Zeisel MB, Blaser E, Schurmann P, Bartosch B, Cosset FL, Patel AH, Meisel H, Baumert J, Viazov S, Rispeter K, Blum HE, Roggendorf M, Baumert TF.** 2007. Rapid induction of virus-neutralizing antibodies and viral clearance in a single-source outbreak of hepatitis C. Proc. Natl. Acad. Sci. U. S. A. **104**:6025–6030.
15. **Law M, Maruyama T, Lewis J, Giang E, Tarr AW, Stamataki Z, Gastaminza P, Chisari FV, Jones IM, Fox RI, Ball JK, McKeating JA, Kneteman NM, Burton DR.** 2008. Broadly neutralizing antibodies protect against hepatitis C virus quasispecies challenge. Nat. Med. **14**:25–27.
16. **Vanwolleghem T, Bukh J, Meuleman P, Desombere I, Meunier JC, Alter H, Purcell RH, Leroux-Roels G.** 2008. Polyclonal immunoglobulins from a chronic hepatitis C virus patient protect human liver-chimeric mice from infection with a homologous hepatitis C virus strain. Hepatology **47**:1846–1855.
17. **Meuleman P, Bukh J, Verhoye L, Farhoudi A, Vanwolleghem T, Wang RY, Desombere I, Alter H, Purcell RH, Leroux-Roels G.** 2011. In vivo evaluation of the cross-genotype neutralizing activity of polyclonal antibodies against hepatitis C virus. Hepatology **53**:755–762.
18. **Halliday J, Klenerman P, Barnes E.** 2011. Vaccination for hepatitis C virus: closing in on an evasive target. Expert Rev. Vaccines **10**:659–672.
19. **Ip PP, Nijman HW, Wilschut J, Daemen T.** 2012. Therapeutic vaccination against chronic hepatitis C virus infection. Antivir. Res. **96**:36–50.
20. **Barnes E, Folgori A, Capone S, Swadling L, Aston S, Kurioka A, Meyer J, Huddart R, Smith K, Townsend R, Brown A, Antrobus R, Ammendola V, Naddeo M, O'Hara G, Willberg C, Harrison A, Grazioli F, Esposito ML, Siani L, Traboni C, Oo Y, Adams D, Hill A, Colloca S, Nicosia A, Cortese R, Klenerman P.** 2012. Novel adenovirus-based vaccines induce broad and sustained T cell responses to HCV in man. Sci. Transl. Med. **4**:115ra1.
21. **Abraham JD, Himoudi N, Kien F, Berland JL, Codran A, Bartosch B, Baumert T, Paranhos-Baccala G, Schuster C, Inchauspe G, Kieny MP.** 2004. Comparative immunogenicity analysis of modified vaccinia Ankara vectors expressing native or modified forms of hepatitis C virus E1 and E2 glycoproteins. Vaccine **22**:3917–3928.
22. **El-Gogo S, Staib C, Lasarte JJ, Sutter G, Adler H.** 2008. Protective vaccination with hepatitis C virus NS3 but not core antigen in a novel mouse challenge model. J. Gene Med. **10**:177–186.
23. **Fournillier A, Gerossier E, Evlashev A, Schmitt D, Simon B, Chatel L, Martin P, Silvestre N, Balloul JM, Barry R, Inchauspe G.** 2007. An accelerated vaccine schedule with a poly-antigenic hepatitis C virus MVA-based candidate vaccine induces potent, long lasting and in vivo cross-reactive T cell responses. Vaccine **25**:7339–7353.
24. **Rollier C, Depla E, Drexhage JA, Verschoor EJ, Verstrepen BE, Fatmi A, Brinster C, Fournillier A, Whelan JA, Whelan M, Jacobs D, Maertens G, Inchauspe G, Heeney JL.** 2004. Control of heterologous hepatitis C virus infection in chimpanzees is associated with the quality of vaccine-induced peripheral T-helper immune response. J. Virol. **78**:187–196.
25. **Habersetzer F, Honnet G, Bain C, Maynard-Muet M, Leroy V, Zarski JP, Feray C, Baumert TF, Bronowicki JP, Doffoel M, Trepo C, Agathon D, Toh ML, Baudin M, Bonnefoy JY, Limacher JM, Inchauspe G.** 2011. A poxvirus vaccine is safe, induces T-cell responses, and decreases viral load in patients with chronic hepatitis C. Gastroenterology **141**:890–899.
26. **Gomez CE, Vandermeeren AM, Garcia MA, Domingo-Gil E, Esteban M.** 2005. Involvement of PKR and RNase L in translational control and induction of apoptosis after hepatitis C polyprotein expression from a vaccinia virus recombinant. Virol. J. **2**:81.
27. **Moradpour D, Penin F, Rice CM.** 2007. Replication of hepatitis C virus. Nat. Rev. Microbiol. **5**:453–463.
28. **Moradpour D, Brass V, Bieck E, Friebe P, Gosert R, Blum HE, Bartenschlager R, Penin F, Lohmann V.** 2004. Membrane association of the RNA-dependent RNA polymerase is essential for hepatitis C virus RNA replication. J. Virol. **78**:13278–13284.
29. **Ramirez JC, Gherardi MM, Esteban M.** 2000. Biology of attenuated modified vaccinia virus Ankara recombinant vector in mice: virus fate and activation of B- and T-cell immune responses in comparison with the Western Reserve strain and advantages as a vaccine. J. Virol. **74**:923–933.
30. **Vandermeeren AM, Gomez CE, Patino C, Domingo-Gil E, Guerra S, Gonzalez JM, Esteban M.** 2008. Subcellular forms and biochemical events triggered in human cells by HCV polyprotein expression from a viral vector. Virol. J. **5**:102.
31. **Delaloye J, Roger T, Steiner-Tardivel QG, Le Roy D, Knaup Reymond M, Akira S, Petrilli V, Gomez CE, Perdiguero B, Tschopp J, Pantaleo G, Esteban M, Calandra T.** 2009. Innate immune sensing of modified vaccinia virus Ankara (MVA) is mediated by TLR2-TLR6, MDA-5, and the NALP3 inflammasome. PLoS Pathog. **5**:e1000480. doi:10.1371/journal.ppat.1000480.
32. **Blom KG, Qazi MR, Matos JB, Nelson BD, DePierre JW, Abedi-Valugerdi M.** 2009. Isolation of murine intrahepatic immune cells employing a modified procedure for mechanical disruption and functional characterization of the B, T, and natural killer T cells obtained. Clin. Exp. Immunol. **155**:320–329.
33. **Garcia-Arriaza J, Najera JL, Gomez CE, Sorzano CO, Esteban M.** 2010. Immunogenic profiling in mice of a HIV/AIDS vaccine candidate (MVA-B) expressing four HIV-1 antigens and potentiation by specific gene deletions. PLoS One **5**:e12395. doi:10.1371/journal.pone.0012395.
34. **Najera JL, Gomez CE, Garcia-Arriaza J, Sorzano CO, Esteban M.** 2010. Insertion of vaccinia virus C7L host range gene into NYVAC-B genome potentiates immune responses against HIV-1 antigens. PLoS One **5**:e11406. doi:10.1371/journal.pone.0011406.
35. **Roederer M, Nozzi JL, Nason MC.** 2011. SPICE: exploration and analysis of post-cytometric complex multivariate datasets. Cytometry A **79**:167–174.
36. **Sillanpaa M, Melen K, Porkka P, Fagerlund R, Nevalainen K, Lappalainen M, Julkunen I.** 2009. Hepatitis C virus core, NS3, NS4B, and NS5A are the major immunogenic proteins in humoral immunity in chronic HCV infection. Virol. J. **6**:84.
37. **Bachmann MF, Wolint P, Schwarz K, Jager P, Oxenius A.** 2005. Functional properties and lineage relationship of $CD8^+$ T cell subsets identified by expression of IL-7 receptor alpha and CD62L. J. Immunol. **175**:4686–4696.
38. **Himoudi N, Abraham JD, Fournillier A, Lone YC, Joubert A, Op De Beeck A, Freida D, Lemonnier F, Kieny MP, Inchauspe G.** 2002. Comparative vaccine studies in HLA-A2.1-transgenic mice reveal a clustered organization of epitopes presented in hepatitis C virus natural infection. J. Virol. **76**:12735–12746.
39. **Gomez CE, Najera JL, Krupa M, Perdiguero B, Esteban M.** 2011. MVA and NYVAC as vaccines against emergent infectious diseases and cancer. Curr. Gene Ther. **11**:189–217.
40. **Paoletti E.** 1996. Applications of pox virus vectors to vaccination: an update. Proc. Natl. Acad. Sci. U. S. A. **93**:11349–11353.
41. **Tester I, Smyk-Pearson S, Wang P, Wertheimer A, Yao E, Lewinsohn DM, Tavis JE, Rosen HR.** 2005. Immune evasion versus recovery after acute hepatitis C virus infection from a shared source. J. Exp. Med. **201**:1725–1731.
42. **Alvarez-Lajonchere L, Shoukry NH, Gra B, Amador-Canizares Y, Helle F, Bedard N, Guerra I, Drouin C, Dubuisson J, Gonzalez-Horta EE, Martinez G, Marante J, Cinza Z, Castellanos M, Duenas-Carrera S.** 2009. Immunogenicity of CIGB-230, a therapeutic DNA vaccine prepara-

tion, in HCV-chronically infected individuals in a phase I clinical trial. J. Viral Hepat. **16**:156–167.
43. **Drane D, Maraskovsky E, Gibson R, Mitchell S, Barnden M, Moskwa A, Shaw D, Gervase B, Coates S, Houghton M, Basser R.** 2009. Priming of $CD4^+$ and $CD8^+$ T cell responses using a HCV core ISCOMATRIX vaccine: a phase I study in healthy volunteers. Hum. Vaccin. **5**:151–157.
44. **Frey SE, Houghton M, Coates S, Abrignani S, Chien D, Rosa D, Pileri P, Ray R, Di Bisceglie AM, Rinella P, Hill H, Wolff MC, Schultze V, Han JH, Scharschmidt B, Belshe RB.** 2010. Safety and immunogenicity of HCV E1E2 vaccine adjuvanted with MF59 administered to healthy adults. Vaccine **28**:6367–6373.
45. **Leroux-Roels G, Depla E, Hulstaert F, Tobback L, Dincq S, Desmet J, Desombere I, Maertens G.** 2004. A candidate vaccine based on the hepatitis C E1 protein: tolerability and immunogenicity in healthy volunteers. Vaccine **22**:3080–3086.
46. **Gowans EJ, Roberts S, Jones K, Dinatale I, Latour PA, Chua B, Eriksson EM, Chin R, Li S, Wall DM, Sparrow RL, Moloney J, Loudovaris M, Ffrench R, Prince HM, Hart D, Zeng W, Torresi J, Brown LE, Jackson DC.** 2010. A phase I clinical trial of dendritic cell immunotherapy in HCV-infected individuals. J. Hepatol. **53**:599–607.
47. **Klade CS, Wedemeyer H, Berg T, Hinrichsen H, Cholewinska G, Zeuzem S, Blum H, Buschle M, Jelovcan S, Buerger V, Tauber E, Frisch J, Manns MP.** 2008. Therapeutic vaccination of chronic hepatitis C non-responder patients with the peptide vaccine IC41. Gastroenterology **134**: 1385–1395.
48. **Schlaphoff V, Klade CS, Jilma B, Jelovcan SB, Cornberg M, Tauber E, Manns MP, Wedemeyer H.** 2007. Functional and phenotypic characterization of peptide-vaccine-induced HCV-specific $CD8^+$ T cells in healthy individuals and chronic hepatitis C patients. Vaccine **25**:6793–6806.
49. **Ward S, Lauer G, Isba R, Walker B, Klenerman P.** 2002. Cellular immune responses against hepatitis C virus: the evidence base 2002. Clin. Exp. Immunol. **128**:195–203.
50. **Buonaguro L, Petrizzo A, Tornesello ML, Buonaguro FM.** 2012. Innate immunity and hepatitis C virus infection: a microarray's view. Infect. Agents Cancer **7**:7.
51. **Lechner F, Wong DK, Dunbar PR, Chapman R, Chung RT, Dohrenwend P, Robbins G, Phillips R, Klenerman P, Walker BD.** 2000. Analysis of successful immune responses in persons infected with hepatitis C virus. J. Exp. Med. **191**:1499–1512.
52. **Smyk-Pearson S, Tester IA, Lezotte D, Sasaki AW, Lewinsohn DM, Rosen HR.** 2006. Differential antigenic hierarchy associated with spontaneous recovery from hepatitis C virus infection: implications for vaccine design. J. Infect. Dis. **194**:454–463.
53. **Grakoui A, Shoukry NH, Woollard DJ, Han JH, Hanson HL, Ghrayeb J, Murthy KK, Rice CM, Walker CM.** 2003. HCV persistence and immune evasion in the absence of memory T cell help. Science **302**:659–662.
54. **Lamonaca V, Missale G, Urbani S, Pilli M, Boni C, Mori C, Sette A, Massari M, Southwood S, Bertoni R, Valli A, Fiaccadori F, Ferrari C.** 1999. Conserved hepatitis C virus sequences are highly immunogenic for $CD4^+$ T cells: implications for vaccine development. Hepatology **30**: 1088–1098.
55. **Lauer GM, Lucas M, Timm J, Ouchi K, Kim AY, Day CL, Schulze Zur Wiesch J, Paranhos-Baccala G, Sheridan I, Casson DR, Reiser M, Gandhi RT, Li B, Allen TM, Chung RT, Klenerman P, Walker BD.** 2005. Full-breadth analysis of $CD8^+$ T-cell responses in acute hepatitis C virus infection and early therapy. J. Virol. **79**:12979–12988.
56. **Neveu B, Debeaupuis E, Echasserieau K, le Moullac-Vaidye B, Gassin M, Jegou L, Decalf J, Albert M, Ferry N, Gournay J, Houssaint E, Bonneville M, Saulquin X.** 2008. Selection of high-avidity CD8 T cells correlates with control of hepatitis C virus infection. Hepatology **48**:713–722.
57. **Boson B, Granio O, Bartenschlager R, Cosset FL.** 2011. A concerted action of hepatitis C virus p7 and nonstructural protein 2 regulates core localization at the endoplasmic reticulum and virus assembly. PLoS Pathog. **7**:e1002144. doi:10.1371/journal.ppat.1002144.
58. **van Leeuwen EM, de Bree GJ, ten Berge IJ, van Lier RA.** 2006. Human virus-specific $CD8^+$ T cells: diversity specialists. Immunol. Rev. **211**:225–235.